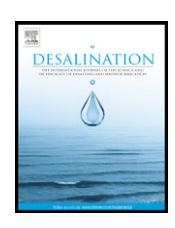


Contents lists available at ScienceDirect

# Desalination

journal homepage: www.elsevier.com/locate/desal



# Feasibility study and performance assessment for the integration of a steam-injected gas turbine and thermal desalination system



Iman Janghorban Esfahani, ChangKyoo Yoo\*

Dept. of Environmental Science and Engineering, College of Engineering, Center for Environmental Studies, Kyung Hee University, Seocheon-dong 1, Giheung-gu, Yongin-Si, Gyeonggi-Do 446-701, Republic of Korea

#### HIGHLIGHTS

- Development of thermodynamic, economic, and environmental models for a SIGT-METVC
- Suggestion of performance criteria for retrofitting the SIGT with METVC
- Feasibility study for retrofitting the SIGT plant with a METVC system using RSM
- · Multi-objective optimization for minimizing the retrofitted unit product cost

#### ARTICLE INFO

Article history:
Received 1 August 2013
Received in revised form 18 October 2013
Accepted 19 October 2013
Available online 10 November 2013

Keywords:
Desalination
Feasibility study
METVC
RSM
Optimization
Retrofitting
SIGT

#### ABSTRACT

This study proposes a systematic approach for retrofitting a steam-injection gas turbine (SIGT) with a multi-effect thermal vapor compression (METVC) desalination system. The retrofitted unit's product cost of the fresh water (RUPC) was used as a performance criterion, which comprises the thermodynamic, economic, and environmental attributes when calculating the total annual cost of the SIGT-METVC system. For the feasibility study of retrofitting the SIGT plant with the METVC desalination system, the effects of two key parameters were analyzed using response surface methodology (RSM) based on a central composite design (CCD): the steam air ratio (SR) and the temperature difference between the effects of the METVC system ( $\Delta T_{METVC}$ ) on the fresh water production ( $Q_{treshwater}$ ) and the net power generation ( $W_{net}$ ) of the SIGT-METVC system. Multi-objective optimization (MOO) which minimizes the modified total annual cost (MTAC) and maximizes the fresh water flow rate was performed to optimize the RUPC of the SIGT-METVC system. The best Pareto optimal solution showed that the SIGT-METVC system with five effects is the best one among the systems with 4–6 effects. This system under optimal operating conditions can save 21.07% and 9.54% of the RUPC, compared to the systems with four and six effects, respectively.

 $\hbox{@ 2013}$  Elsevier B.V. All rights reserved.

# 1. Introduction

To overcome the scarcity of power and fresh water, thermal desalination plants are usually integrated with power plants as a dual-purpose system for the simultaneous production of power and fresh water. These are generally more profitable, economically, and in terms of energy efficiency compared to standalone power plants and thermal desalination systems [1,2]. Among power plants, humidified gas turbines (HGT), which use a gas water mixture as the working fluid, have higher efficiency and specific power output with lower specific investment costs and  $NO_{\rm x}$  emissions, compared to other power generation cycles. For a given power generation, the injection of steam in the combustion chamber decreases the fuel consumption, which results in an increase in the thermal efficiency and vice versa for a given fuel

consumption, resulting in increased power generation. The steaminjection contributes to pollutant emissions from the SIGT system depending on the adiabatic flame temperature. The amount of Carbone monoxide (CO) and nitrogen oxides (NO $_{\rm x}$ ) produced in the combustion chamber and combustion reaction are mainly a function of the adiabatic flame temperature, which is the temperature reached by burning a theoretically correct mixture of fuel and air in an isolated vessel [1,3]. Increasing the adiabatic flame temperature increases the thermal NO $_{\rm x}$  formed from the oxidation of the free nitrogen in the combustion air or fuel. However, the CO emission decreases when the adiabatic flame temperature increases.

There are several configurations of HGT cycles, including the steam-injected gas turbine (SIGT) cycle, humid air turbine (HAT), and evaporative gas turbine (EvGT) [3]. In a SIGT system, steam is generated using a heat recovery steam generator (HRSG), injected into the gas turbine combustion chamber and utilized as working-fluid with air [4]. Recently, several studies have examined injected-steam gas turbines [2–12].

<sup>\*</sup> Corresponding author. E-mail address: ckyoo@khu.ac.kr (C.K. Yoo).

Paepe and Dick [6] analyzed the water recovery in steam injected gas turbines in terms of the technology and economy. Nishida et al. [4] analyzed the performance characteristics of two types of regenerative steam-injection gas-turbines and compared their performance with that of simple, regenerative, water injection and steam injected gasturbine cycles. They showed that the steam-injection configuration can be applied in a flexible heat-and-power cogeneration system. Wang and Lior [3] investigated the performance of a SIGT-based combined system with thermal desalination systems. Their analysis improved our understanding of the combined SIGT power and water desalination process and showed ways to improve and optimize it.

The SIGT systems are available as combined heat and power (CHP) systems, producing heat and power simultaneously. Since the major disadvantage of SIGT systems is their large water consumption, especially in water-short areas, these systems are usually integrated with thermal desalination systems, such as multi-effect thermal-vapor compression (METVC), to produce fresh water for the power cycle and other productions. In order to assess the combination of SIGT systems and thermal desalination systems, several performance criteria, based on thermodynamics and economics, have been defined in the literature [7,13,14]. Agarwal et al. [7] improved the performance of a simple gas turbine cycle through the integration of inlet air evaporative cooling and steam injection using thermal efficiency and exergy efficiency as their two thermodynamic performance criteria. Shakouri et al. [14] studied the feasibility of a dual purpose system using the unit product cost of fresh water as a performance criterion, based on economic analysis. In combined SIGT and desalination systems, since the steaminjection process effects the thermal efficiency (fuel consumption), power generation, pollutant emissions and water production, the thermodynamic, economic and environmental aspects should all be taken into consideration in order to define a performance criterion for assessing the retrofitting of a SIGT plant with a thermal desalination

As seen in our literature review, recent research efforts have focused on defining the performance criteria based on either thermodynamics or economics, without considering the environmental aspect. This study proposes a systematic approach to define a performance criterion for retrofitting a SIGT plant using a thermal desalination system. Since the main purpose of integrating a SIGT plant with a thermal desalination system is to produce fresh water, in this study the integration of the systems is assessed based on the fresh water production costs. In order to consider the thermodynamic and environmental aspects of the SIGT and METVC integration, we defined two costs: the lost opportunity costs and the found opportunity costs. These contribute to decreases in the total annual costs (TAC). The TAC of the retrofitted SIGT with a METVC system was modified by adding the lost opportunity costs and subtracting the found opportunity costs. The retrofitted unit product cost (RUPC) of the fresh water, as an efficient performance criterion for retrofitting a SIGT plant with a METVC system, which considers both the thermodynamic and environmental impacts of the integration process, was defined by dividing the MTAC by the fresh water production.

This paper consists of four major parts. First, we developed theoretical models, including thermodynamic and environmental models, to calculate the power generation and fresh water production of the retrofitted SIGT–METVC system. In addition, we developed an economic model used to calculate the unit product cost of the fresh water, which includes the lost opportunity and found opportunity costs in the total annual costs of the retrofitted SIGT–METVC system. Second, we determined the sensitivity analysis and feasibility study to assess the retrofitting possibility of the SIGT plant with METVC desalination system, specifically investigating the effect of two key parameters: the temperature difference between effects in the METVC system ( $\Delta T_{\text{MED-TVC}}$ ) and steam air ratio (SR) on the fresh water flow rate  $Q_{\text{freshwater}}$  and the net power generation ( $W_{\text{net}}$ ) of the retrofitted using system response surface methodology (RSM). Third, we optimized the RUPC

of the fresh water as a new performance criterion for retrofitting the SIGT plants using multi-objective optimization (MOO), which maximizes the Q<sub>freshwater</sub> and minimizes the MTAC of the retrofitted system. We obtained Pareto optimal fronts as a set of optimal solutions, selecting the one which best corresponded to the minimum value of the RUPC.

#### 2. Material and methods

#### 2.1. System configuration

Fig. 1 shows a schematic of a retrofitted SIGT plant with a METVC desalination system [3]. The SIGT subsystem includes a gas turbine power plant and a heat recovery steam generator (HRSG). In the GT subsystem, air is compressed by an air compressor. The compressed air is sent to the combustion chamber (CC) where the fuel and steam are injected. The hot gas from the CC is expanded through the GT, where the shaft work is generated to operate an air compressor and a generator. The expanded gas passes through a HRSG to recover the waste heat of the exhaust gas in order to produce saturated steam as motive steam for the METVC system and superheated steam to inject into the combustion chamber.

The detailed schematic of the METVC desalination system with n effects is shown in Fig. 2 [13]. The motive steam, generated by HRSG, was used by a steam jet ejector (SJE) to compress some of the water vapor produced by the last effect. The compressed vapor was introduced into the tube side in the first effect and condensed by releasing its latent heat into the feed water for evaporation. A part of the condensate returns to the HRSG, with the other part passing into the first flashing box. Demisted vapor that forms during the first effect and the flashed vapor from the first flashing box are used together as heating sources in the first pre-heater in order to preheat the feed water to the first effect. The combined vapor from the first pre-heater passes into the second effect and is used as the heat source to vaporize the feed water in the second effect. This process is repeated for all of the effects until the last one, where the vapor generated from the last effect is condensed through the condenser.

#### 2.2. Thermodynamic and economic modeling

In this section we detail the equations that form the thermodynamic and economic models for the SIGT–METVC system presented in Figs. 1 and 2. The models, developed by Janghorban Esfahani et al. [13,15], Wang and Lior [16] were used for thermodynamic modeling and the models, developed by Lazzaretto and Toffolo [17], Cardu and Baica [9], Janghorban Esfahani et al. [13] and Rossen et al. [18], were used for our economic model. Several simplifying assumptions, listed below, were used in the development of our thermodynamic model:

- The cogeneration systems are operated under steady-state conditions;
- The principle of the ideal-gas mixture is applied to the air and combustion products;
- The dead state condition is  $P_0 = 1.01$  bar and  $T_0 = 25$  °C;
- The temperature differences across the feed heaters are equal, in order to achieve the optimum operating conditions in the METVC desalination system;
- The feed flow rate for all of the effects is equal in the METVC desalination system;

The governing equations for the thermodynamic modeling (presented in Tables 1A to 4A) and for the economic modeling (presented in Table 1B and Eqs. (B18) to (B 23)) of the SIGT subsystem and METVC subsystem were developed using Matlab software in order to simulate the combined system. In this study, we considered the system presented in Table 1 as a SIGT plant [2]. The thermodynamic parameter's initial conditions for the METVC desalination system are presented in Table 2. The simulated models were validated by

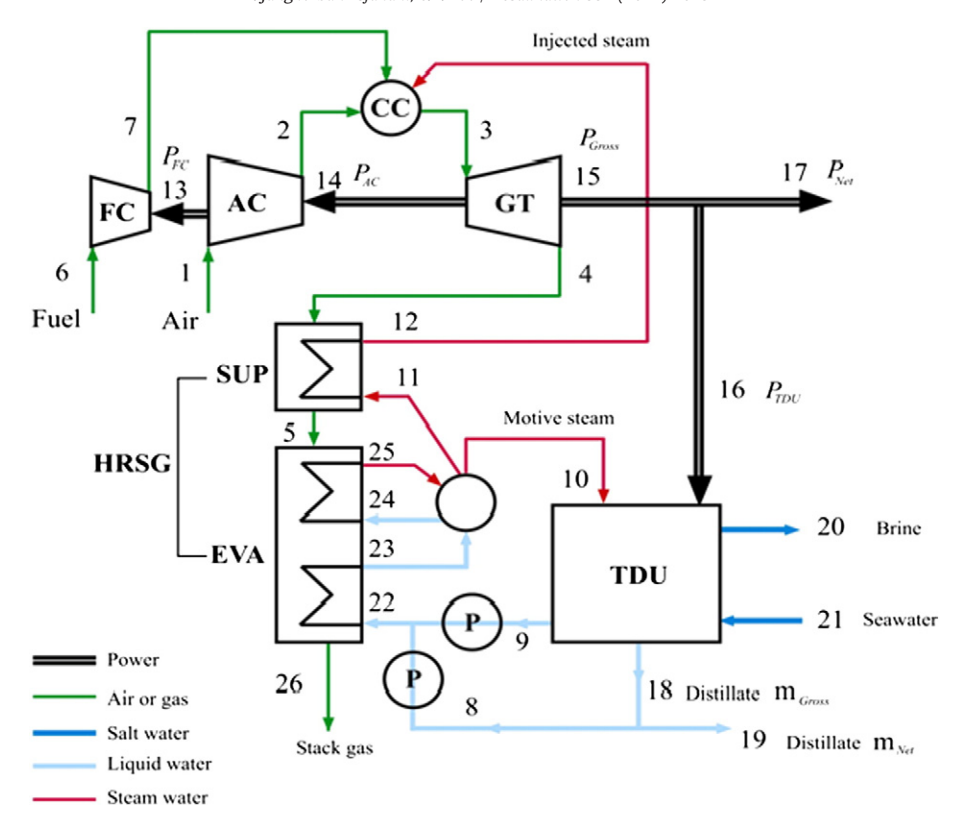


Fig. 1. Schematic of a retrofitted SIGT with a METVC desalination system [3].

comparing the simulation results of the SIGT and METVC systems with those found in the relevant literature [2,18] under the same conditions (for example, the relative errors of the net power generation of the SIGT and gain output ratio of the METVC desalination system were both within 2.75%).

# 2.3. Environmental analysis

The toxic emissions, such as CO and  $NO_x$ , are undesired products of the energy conversion process, which are produced with desired products such as power, heat, and water [7]. The thermal  $NO_x$ , which is the oxidation of the free nitrogen in the combustion air or fuel, is

primarily a function of the adiabatic flame temperature. The adiabatic flame temperature in the primary zone of the combustion chamber is given by Eq. (1) [17,19]:

$$T_{pz} = A \cdot \sigma^{\alpha} \cdot \exp(\beta \cdot (\sigma + \lambda)^{2}) \cdot \pi^{x^{*}} \cdot \theta^{y^{*}} \cdot \psi^{z^{*}}$$
 (1)

where  $\pi$  is dimensionless pressure (P/P<sub>ref</sub>),  $\theta$  is dimensionless temperature (T/T<sub>ref</sub>), and  $\psi$  is the H/C atomic ratio, which is equal to four for pure methane.  $\sigma$  is calculated by Eq. (2) [17]:

$$\sigma = \begin{cases} = \phi & \text{for } \phi \leq 1 \\ = \phi - 0.7 & \text{for } \phi \geq 1 \end{cases} \tag{2}$$

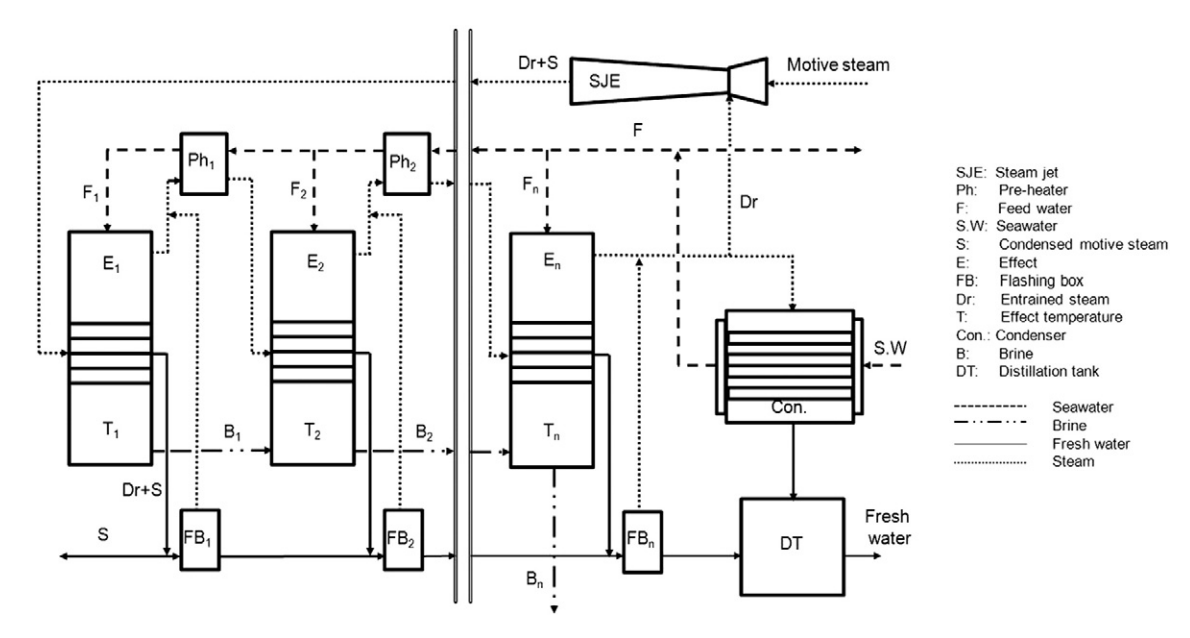


Fig. 2. Schematic of a METVC desalination system [13].

**Table 1**Specifications of the SIGT power plant [2].

Parameters	Value
Pressure ratio	30
Turbine inlet temperature	1300 °C
Inlet air temperature	25 °C
Fuel	Methane
Combustor efficiency	0.99
Compressor efficiency	0.88
Turbine efficiency	0.9
Minimum pinch point temperature in HRSG	15
Pressure of injected steam	3500 kpa
Mass ratio of injected steam and compressed air (SR)	0.07
Fuel mass flow rate	0.0203 kg/s
Air mass flow rate	1 kg/s
Net power generation	515 kW

where  $\varphi$  is the mass or molar ratio.In addition, x, y, and z are the quadratic functions of  $\sigma$  based on the Eqs. (3) to (5) [17].

$$x^* = a_1 + b_1 \cdot \sigma + c_1 \cdot \sigma^2 \tag{3}$$

$$y^* = a_2 + b_2 \cdot \sigma + c_2 \cdot \sigma^2 \tag{4}$$

$$z^* = a_3 + b_3^3 \sigma + c_3 \cdot \sigma^2 \tag{5}$$

where A,  $\alpha$ ,  $\beta$ ,  $\lambda$ ,  $a_i$ ,  $b_i$ , and  $c_i$  are constants. The values of these parameters are listed in Table 3. [17].

The amounts of CO and  $NO_x$  produced in a combustion chamber and combustion reaction depends on the adiabatic flame temperature. The CO and  $NO_x$  pollutant emissions (in grams per kilogram of fuel) are determined by Eqs. (6) and (7), respectively [17]:

$$m_{NOX} = \frac{0.15E16 \cdot \tau^{0.5} \cdot \exp\left(-71100/T_{pz}\right)}{P_3^{0.05} \cdot \left(\frac{\Delta P_3}{P_3}\right)^{0.5}} \tag{6}$$

$$CO = \frac{0.18E9 \cdot \exp\left(7800/T_{pz}\right)}{P_3^2 \cdot \tau \cdot \left(\frac{\Delta P_3}{P_3}\right)^{0.5}}$$
(7)

where  $\tau$  is the residence time in the combustion zone (assumed constant and equal to 0.002 s),  $T_{pz}$  is the primary zone combustion temperature,  $P_3$  is the combustor inlet pressure, and  $\Delta P_3/P_3$  is the non-dimensional pressure drop in the combustion chamber.

# 2.4. Cost performance criteria definition

Since the main purpose of retrofitting the SIGT systems with thermal desalination systems is fresh water production, a performance criterion that considers all of the effects of the integration with fresh water production is needed in order to assess these effects. In the retrofitted SIGT plant with thermal desalination systems, the steam-injection process effects the thermal efficiency (fuel consumption), power generation, pollutant emissions and water production; therefore, in order to define a performance criterion, the thermodynamic, economic and environmental aspects should all be considered.

 Table 2

 Thermodynamic parameter's initial circumstances for METVC desalination system [13].

Parameter	Value	Unit
Salinity of seawater	36,000	ppm
Salinity of last effect brine	70,000	ppm
Temperature of seawater	25	°C
Pressure of seawater	1	bar
Top brine temperature	69	°C
Boiling point elevation	0.8	_

**Table 3** Constants for Eqs. (3)–(5) [17].

Constants	$0.3 \le \varphi \le 1.0$		$1.0 \le \varphi \le 1.6$	
	$0.92 \le \theta \le 2$	$2 \le \theta \le 3.2$	$0.92 \le \theta \le 2$	$2 \le \theta \le 3.2$
A	2361.7644	2315.752	916.8216	1246.1778
α	0.1157	-0.0493	0.2885	0.3819
β	-0.9489	-1.1141	0.1456	0.3479
λ	-1.0976	-1.1807	-3.2771	-2.0365
$a_1$	0.0143	0.0106	0.0311	0.0361
$b_1$	-0.0553	-0.045	-0.078	-0.085
$c_1$	0.0526	0.0482	0.0497	0.0517
$a_2$	0.3955	0.5688	0.0254	0.0097
$b_2$	-0.4417	-0.55	0.2602	0.502
$c_2$	0.141	0.1319	-0.1318	-0.2471
$a_3$	0.0052	0.0108	0.0042	0.017
$b_3$	-0.1289	-0.1291	-0.1781	-0.1894
C <sub>3</sub>	0.0827	0.0848	0.098	0.1037

The conventional performance criterion for retrofitting the SIGT plant with thermal desalination systems is the unit product cost of the fresh water (UPC<sub>fresh water</sub>), which is calculated using Eq. (8):

$$UPC_{Fresh water} = \frac{TAC_{METVC}}{Q_{Fresh water}} \qquad \left(/m^3\right)$$
 (8)

where  $TAC_{METVC}$  is the total annual cost of the METVC, which calculated using Eq. (9) and  $Q_{freshwater}$  is fresh water production of the SIGT–METVC system.

$$TAC_{METVC} = ACC_{METVC} + AOC_{METVC}$$
(9)

where  $ACC_{METVC}$  is the annual capital cost of the METVC system and  $AOC_{METVC}$  is the annual operating cost of the METVC system.

Thermal energy cost accounts for a large part of the TAC which should be considered as a part of the annual operating cost. Because the variations of the SR,  $\Delta T_{METVC}$  and number of effects in METVC system cause the variations of the fuel mass flow rate, the variations of the fuel mass flow rate should be considered in annual operating cost calculation. Thermal energy cost for integrated SIGT with METVC system is calculated by Eq. (10)

$$C_{th} = \left( \dot{\eta}_{tuel} - 0.0203 \right) \cdot LHV \cdot f \cdot 365 \cdot C_{fuel}$$
 (10)

where  $C_{th}$  and  $m_{fuel}$  are thermal energy cost and fuel mass flow rate of the integrated system respectively, LHV is low heating value of fuel, f is load factor, and  $C_{fuel}$  is fuel cost which is considered as 0.003 \$/MW [21]. In order to calculate the energy thermal cost of the integrated system the fuel mass flow rate of the integrated system ( $m_{fuel}$ ) should be subtracted by fuel mass flow rate of the stand alone SIGT power plant which is 0.0203 kg/s. Specific thermal energy cost of fresh water (STECFW) as an energy performance criterion for retrofitted system is calculated by Eq. (11).

$$STECFW = C_{th} \cdot Q_{fresh-water}$$
 (11)

In the retrofitted SIGT plant with a METVC system, since a portion of the water is consumed for the steam-injection process, increasing the steam air ratio (SR) decreases the net fresh water production while increasing the net power generation. In addition to an increase in the SR due to a decreased adiabatic flame temperature, the  $NO_x$  emission decreases as the CO emissions increase. Thus, increasing the fresh water production corresponds to a power generation reduction, CO emission reduction, and  $NO_x$  emission increase. In the other words, increasing the fresh water production causes a loss of opportunities for power generation and  $NO_x$  reduction, while simultaneously enabling opportunities for CO reduction. Fig. 3 shows the effect of the SR on the net power generation and fresh water production of the SIGT–METVC

system. As shown in Fig. 3, for a given value of the fresh water production, power generation opportunities are lost by  $\Delta Power$ , which could be generated by consuming all of the fresh water produced by the METVC system.

Fig. 4 shows the effect of the SR on the CO and  $NO_x$  emissions. For a given SR value, which corresponds to a given value of fresh water production, the opportunity for  $NO_x$  reduction is lost by  $\Delta NO_x$  and the opportunity for CO reduction is enabled by  $\Delta CO$ . This lost opportunity for NOx reduction can be decreased by reducing the fresh water production. And the opportunity for CO reduction can be increased by improving the fresh water production.

Since CO and  $NO_x$  emissions can be expressed by the pollution damage cost [17] and power generation can be expressed by income resulting from the sale of the generated power, the aforementioned opportunities are expressed in terms of cost. The lost opportunity cost of power generation is given by Eq. (12):

$$LOCPG = \Delta Power \cdot SP_{power} \cdot 24 \cdot 365 \cdot f \tag{12}$$

where *LOCPG* is the lost opportunity cost of the power generation,  $\Delta Power$  is the lost opportunity of power generation,  $SP_{power}$  is the sale price of the power generated, and f is the plant load factor.

The lost opportunity cost of  $NO_x$  reduction is expressed by Eq. (13).

$$LOCNOx = \Delta NO_{x} \cdot C_{NO_{x}} \cdot 24 \cdot 365 \cdot f \tag{13}$$

where  $LOCNO_X$  is the lost opportunity cost of the  $NO_X$  reduction,  $\Delta NO_X$  is the lost opportunity resulting from  $NO_X$  reduction,  $C_{NOX}$  is the pollution damage cost of the  $NO_X$  emission, and f is the plant load factor.

The found opportunity cost from the CO reduction is expressed by Eq. (14).

$$FOCCO = \Delta CO \cdot C_{CO} \cdot 24 \cdot 365 \cdot f \tag{14}$$

where *FOCCO* is the found opportunity cost of the *CO* reduction,  $\Delta CO$  is the found opportunity from the *CO* reduction,  $C_{CO}$  is the pollution damage cost of the *CO* emission, and f is the plant load factor.

In order to consider the opportunity costs, which result from the SIGT plant being retrofitted with a METVC system, in terms of the unit product cost of the fresh water (Eq. (8)), the retrofitted unit product cost of the fresh water (RUPC<sub>freshwater</sub>) can be determined using Eq. (15):

$$RUPC_{freshwater} = \frac{RTAC}{Q_{Fresh\ water}} \qquad \left(/m^3\right) \tag{15}$$

where  $RUPC_{freshwater}$  is the retrofitted unit product cost of the fresh water, RTAC is the retrofitted annual cost, and  $Q_{freshwater}$  is the fresh water flow rate. The RTAC is calculated by Eq. (16), which considers

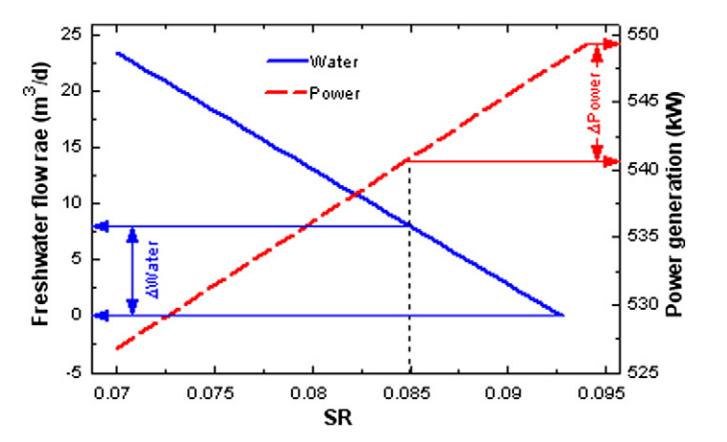


Fig. 3. Effect of steam ratio on power generation and fresh water production.

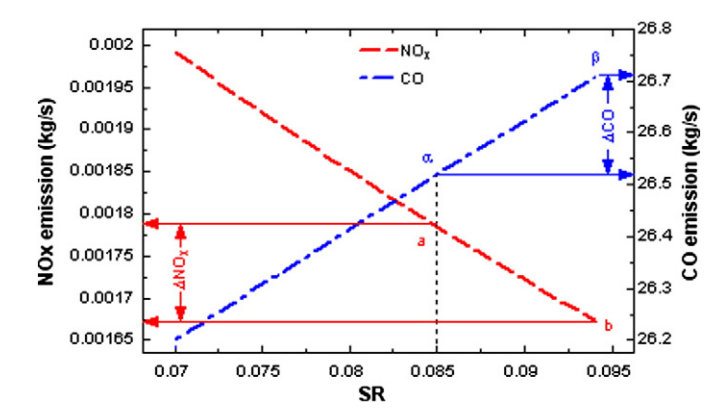


Fig. 4. Effect of SR on NO<sub>x</sub> and CO emissions.

the lost and found opportunity costs of the SIGT-METVC system for the  $TAC_{METVC}$  used in Eq. (8).

$$RTAC = TAC_{METVC} + LOCPG + LOCNO_{x} - FOCCO$$
 (16)

As presented in Eq. (16), since FOCCO decreases the cost of CO emissions. FOCCO was subtracted from the other costs.

# 2.5. Response surface methodology

The response surface methodology (RSM) consists of a group of mathematical and statistical techniques devoted to the evaluation of the relationship between the dependent variable or response (Y) and a set of independent variables or factors  $(X_1,...,X_k)$  [20,22]. The RSM can illustrate the response surface of the dependent variables by varying a number of independent variables or factors, which affect the responses of the dependent variables [23].

When it is assumed that the k number of independent variables,  $X = (X_1, X_2, ..., X_k)$ , affects the p number of response variables,  $Y = (Y_1, Y_2, ..., Y_p)$ , the general function of the response surface method can be represented as Eq. (17).

$$Y_{ii} = f_i(X_1, X_2, ..., X_k), i = 1, 2, ..., pandj = 1, 2, ..., k$$
 (17)

where  $f_i$  is a function between the response variables and the dependent variables. Because  $f_i$  is generally an unknown function, it is assumed that it can be calculated through experimentation [24].

The relationship between the response and the factors is explained by the second-order polynomial regression model shown in Eq. (18) [24].

$$Y = \beta_0 + \sum_{i=1}^{n} \beta_i x_i + \sum_{i=1}^{n} \beta_{ii} x_i^2 + \sum_{i=1}^{n-1} \sum_{j=1}^{n} \beta_{ij} x_i x_j$$
 (18)

where *Y* is the response variable,  $x_i$  and  $x_j$  are the coded levels of the input variables,  $\beta_0$  is the intercept term, and  $\beta_i$ ,  $\beta_{ii}$ , and  $\beta_{ij}$  are the coefficients representing the linear effect, quadratic effect, and interaction effect, respectively, which are known as the regression coefficients.

The significance of the input variables, their interactions, and the goodness of fit of the RSM models were tested using an analysis of variance (ANOVA). An alpha  $(\alpha)$  level of 0.05 was used to determine the statistical significance of all analyses. The significance of each of the coefficients was determined using F-values and P-values. The effect terms with coefficients that had F-values greater than Fisher's F-test values and P-values less than 0.05 were considered to have a high significance on the RSM models. Fisher's F-test was calculated by Eq. (19) using MATLAB software:

$$Fisher'sF - test = F_{\alpha,df,(n-df+1)}$$

$$\tag{19}$$

where  $\alpha$ , df and n are the desired probability level, degree of freedom and observations, respectively.

The goodness of fit of the RSM models was tested using the multiple correlation coefficients ( $R^2$ ). If the  $R^2$  is closer to unity and in agreement with the value of the adjusted multiple correlation coefficient (adj.  $R^2$ ), then the fit of the RSM model is valid.

In this study, RSM models were developed to determine the effects of the two key parameters, SR and  $\Delta T_{METVC}$ , on three responses, W<sub>net</sub>, Q<sub>freshwater</sub> and STECFW. As presented in Table 1, there are other changeable parameters which influence water cost, which are the pressure ratio, the turbine inlet temperature and some other parameters. Because the purpose of this study is to suggest a new systematic approach for retrofitting the SIGT plant with a METVC system, the process parameters of steam air ratio (SR), the pressure ratio, the turbine inlet temperature and some other parameters are considered to be constant although they are changeable and have influence on the fresh water cost. SR is selected as the most significant parameter among all parameters. Note that SR has direct effect on net power generation and water production of the retrofitted SIGT system with METVC. Also  $\Delta T_{METVC}$ and the number of effects were selected as two design parameters of the SIGT-METVC system, since for retrofitting the SIGT system the METVC system should be designed. Furthermore, a feasibility analysis was carried out so as to understand and determine feasible operating conditions for retrofitting a SIGT plant with a METVC desalination system to produce a given amount of fresh water and power. The set of operation conditions in a desalination system were obtained based on the design of experiment (DOE). Since two factors (k=2) including  $\Delta T$  and SR are of interest, a factorial experiment was used. In factorial experience for two factors we need a 2<sup>2</sup> design with center points which is required for first order model as well as 2 K star points. The star or axial points are at some value  $\alpha$  and  $-\alpha$  on each axis. The  $2^2$  design gives a box and adding axial points outside of the box gives a spherical design where  $\alpha = \sqrt{k}$ . The corner points and the axial points at  $\alpha$  are all on the surface of a ball in three dimensions. For central composite design with two factors there are 5 center points. The reason is related to the variance of a predicted value. By picking five center points, the variance in the middle is approximately the same as the variance at the edge. If only there is one or two center points the precision in the middle is less than that of at the edge [24].

The central composite experimental design (CCD) with five level coded input factors (-1.41421, -1, 0, 1, +1.41421) was used in this paper. The designed sets of data obtained by the CCD are presented in Table 4, which are in terms of the coded and actual values of the input variables. The theoretical model equations presented in Tables 1A to 4A were simulated for the values of the inputs specified in the CCD, and the corresponding output variables (W<sub>net</sub>, Q<sub>freshwater</sub> and STECFW) were calculated. The values of the theoretical model outputs are presented in Table 5. These inputs-outputs data were subjected to multiple regressions by RSM using MINITAB 14 software. Some risks in the reliability may come from theoretically calculated single data points instead of experimental data with duplicate as source for analysis. Because the RSM models were used to investigate the feasibility about retrofitting the SIGT with METVC system in this study (not for calculating the key parameters values of the system), the reliability of the feasibility results can be acceptable.

# 2.6. Multi-objective optimization

Multi-objective optimization involves the simultaneous optimization of more than one objective function. Several industrial systems have been optimized over the last two decades with multiple objective functions and constraints, using a variety of algorithms. In such cases, a set of several equally good (non-dominating) solutions or a Pareto front may be generated. The evolutionary genetic algorithm (*GA*) has become quite popular in recent years for solving problems involving multiple objective functions [23]. In the case of multi-objective problems, no

single optimized solution can be achieved, and a search is generally performed following the concept of Pareto-optimality, where a set of solutions are developed, providing the best possible compromises between the objectives. When several conflicting objective functions exist, the concept of "optimum" changes from the unique global optimum, as used in single objective problems, to a set of solutions providing the best possible compromises between the objectives, known as the Pareto front. According to the definition Pareto-optimality, no other solution can exist in the feasible range that is at least as good as some member of the Pareto set, in terms of all of the objectives, and is strictly better in terms of at least one [26].

Since the MOO can achieve a Pareto set, which provide useful insights to decision-makers, we used the MOO to optimize the RUPC of the fresh water, rather than using a single objective function optimization by maximizing the  $Q_{freshwater}$  and minimizing the RTAC. Since the numerator and denominator of Eq. (15) which calculates the RUPC as the RTAC and  $Q_{freshwater}$  respectively, by maximizing the  $Q_{freshwater}$  and minimizing the RTAC, the RUPC can be minimized. Therefore, we used the RTAC and  $Q_{freshwater}$  as the fitness functions for the MOO, using a GA with the 'gamultiobj' function in MATLAB 7.11, and the Pareto optimal solution sets were obtained for a retrofitted SIGT plant with METVC systems with different numbers of effects. The independent variables of these functions were  $\Delta T_{MED-TVC}$ , and SR. The operation ranges of each variable were selected based on the working ranges of the various parameters in the SIGT–METVC system. The constraints of the parameters are summarized in Table 6.

#### 2.6.1. Genetic algorithm

A genetic algorithm (GA) is a parallel, iterative, and populationbased search used to determine the optimal solution in a large solution domain by carrying out stochastic transformations inspired by natural evolution. The basic building blocks of a genetic algorithm are genes that form chromosomes. Each gene controls one or more features of its chromosome. A collection of chromosomes creates a population. With a randomly generated population, the algorithm begins using three genetic operators: selection, crossover, and mutation [27–29]. On the basis of the values of the individuals, the chromosomes are selected for the transition from the current population by means of a selection process known as the selection operator. Based on biological recombination, the crossover operator combines two chromosomes, called parents, to generate two similar children. The crossover operator continues until it completes the generation [25,27,28]. As the selection and crossover may become overzealous, the mutation operator performs random changes in the genes of the existing chromosomes [30,31]. The total processes (selection, crossover, and mutation) are referred to as one generation. The generational cycle will stop when a desired termination criterion has been achieved [32].

GA is used to find a set of multiple non-dominated solutions by modifying a generic single-objective GA as a multi-objective optimization problem. GA has been known as the most popular heuristic approach to MOO problems because first, the crossover operator of GA may exploit structures of good solutions with respect to different objectives to create new non-dominated solutions in unexplored parts of the Pareto front and second, most multi-objective GA do not require the user to prioritize, scale, or weight objectives [33].

In order to obtain the Pareto optimal solution set for each system (with different n's), RTAC and Q<sub>freshwater</sub> were used as the fitness functions of the GA with the 'gamultiobj' function. The population type which specifies the type of the inputs to the fitness function was adjusted to a 'double vector'. The size of the population which specifies the number of individuals in each generation was defined 45. The creation function which creates the initial population was selected as 'uniform' function. The 'uniform' function is a random initial population with a uniform distribution which is used for MOO problem without constraints. The selection function which chooses parents for the next generation based on their scaled values from the fitness functions was

**Table 4** CCD for SIGT–METVC system with 3, 4, 5, and 6 effects.

Set no.		Input variables for METVC system with 3 effects			Input variables for METVC system with 4 effects			Input variables for METVC system with 5 effects			Input variables for METVC system with 6 effects					
X	x <sub>1</sub>	ΔT (°C)	<i>x</i> <sub>2</sub>	SR	x <sub>1</sub>	ΔT (°C)	<i>x</i> <sub>2</sub>	SR	x <sub>1</sub>	ΔT (°C)	<i>x</i> <sub>2</sub>	SR	x <sub>1</sub>	ΔT (°C)	$\chi_2$	SR
1	0	8	0	0.077	0	6	0	0.078	0	5.000	0	0.080	0	4.00	0	0.081
2	1	11.53	1	0.082	1	8.12	1	0.084	1	6.414	1	0.087	1	4.71	1	0.089
3	1.41	13	0	0.077	1.41	9	0	0.078	1.41	7.000	0	0.080	1.41	5.00	0	0.081
4	-1.41	3	0	0.077	-1.41	3	0	0.078	-1.41	3.000	0	0.080	-1.41	3.00	0	0.081
5	0	8	0	0.077	0	6	0	0.078	0	5.000	0	0.080	0	4.00	0	0.081
6	0	8	0	0.077	0	6	0	0.078	0	5.000	0	0.080	0	4.00	0	0.081
7	1	11.53	-1	0.072	1	8.12	-1	0.072	1	6.414	-1	0.073	1	4.71	-1	0.073
8	0	8	0	0.077	0	6	0	0.078	0	5.000	0	0.080	0	4.00	0	0.081
9	-1	4.46	-1	0.072	-1	3.88	-1	0.072	-1	3.585	-1	0.073	-1	3.29	-1	0.073
10	-1	4.46	1	0.082	-1	3.88	1	0.084	-1	3.585	1	0.087	-1	3.29	1	0.089
11	0	8	1.41	0.084	0	6	1.41	0.087	0	5.000	1.41	0.090	0	4.00	1.41	0.093
12	0	8	-1.41	0.07	0	6	-1.41	0.07	0	5.000	-1.41	0.070	0	4.00	-1.41	0.070
13	0	8	0	0.077	0	6	0	0.078	0	5.000	0	0.080	0	4.00	0	0.081

selected as the 'tournament' with the size of 2. 'Tournament' selects each parent by choosing individuals at random, and then choosing the best individual out of that set to be a parent. Mutation function which makes small random changes in the individuals in the population was chosen to be 'adaptive feasible'. Adaptive feasible randomly generates directions that are adaptive with respect to the last successful or unsuccessful generation. Crossover function which combines two individuals or parents to form a new individual or child for the next generation was chosen to be 'Scattered'. The direction, fraction, and interval of migration were set as 'forward', 0.2, and 20, respectively. The distance measure function which is a measure of the concentration of the population and Pareto front population fraction which keeps the most fit population down to the specified fraction were chosen to be 'distance crowding' and 0.35, respectively.

# 2.7. SIGT-METVC system integration framework

The framework for retrofitting the SIGT plant with a METVC system is shown in Fig. 5. First, we developed the theoretical models, including the thermodynamic, economic, and environmental models, in order to calculate the power generation, fresh water production, and pollutant emissions so as to define the retrofitted unit product cost of the fresh water (RUPC $_{\rm freshwater}$ ). Second the experimental design was defined, with  $\Delta T_{\rm MED-TVC}$  and SR as the independent variables and  $W_{\rm net}$  and  $Q_{\rm freshwater}$  as the response variables. The experimental design, using a central composite design (CCD), determines the datasets used to simulate the theoretical models. The corresponding output variables of the designed set data obtained by the CCD were calculated using theoretical models, in terms of actual values. Third, quadratic polynomial

models were developed, based on the RSM, in order to describe the relationship between the independent variables (inputs) and the dependent (responses) and to study the feasibility of the SIGT retrofitting. Forth, multi-objective optimization was carried out in order to optimize the RUPC by minimizing the RTAC and maximizing the Q<sub>freshwater</sub>. The Pareto optimal front was obtained as a set of optimal solutions and the best one was selected based on the minimum value of the RUPC.

#### 3. Results and discussions

#### 3.1. Process analysis by RSM modeling

Since the net power generation is affected by just the SR, the values of the fresh water production ( $Q_{freshwater}$  and STECFW) corresponding to CCD data sets of two input variables ( $\Delta T_{MED-TVC}$  and SR) were obtained for our SIGT system retrofitted by METVC systems with 3, 4, 5 and 6 effects by simulating the theoretical models. The actual and coded values of the input variables of the CCD data sets with the corresponding values of the responses are presented in Tables 4 and 5. Each of the input variables was consecutively coded as  $x_1$  and  $x_2$  at five levels: -1.41421, -1.0.1 and 1.41421.

According to Table 4 and the constraints presented in Table 6, the variations ranges of the  $\Delta T_{METVC}$  for the METVC systems with 3, 4, 5, and 6 effects were from 3 °C to 13 °C, 9 °C, 7 °C and 5 °C, respectively, and the variations range of the SR for SIGT–METVC systems with 3, 4, 5, and 6 effects in the METVC were from 0.07 kg/s to 0.084 kg/s, 0.087 kg/s, 0.09 kg/s, and 0.093 kg/s, respectively. These were defined based on the maximum value of fresh water production by the METVC

**Table 5**Mathematical responses for SIGT–METVC system with 3, 4, 5, and 6 effects.

Set no.	Responses for	Responses for SIGT–METVC										
	With 3 effects	With 3 effects		With 4 effects			With 6 effects					
	$Q(m^3/d)$	STECFW	$Q(m^3/d)$	STECFW	$Q(m^3/d)$	STECFW	$Q(m^3/d)$	STECFW				
1	3.6490	0.0017590	6.9910	0.0014620	9.7150	0.0014610	11.5600	0.0015620				
2	1.0530	0.0043170	2.9850	0.0031300	4.0310	0.0030480	4.3170	0.0032010				
3	4.4330	0.0016020	8.0120	0.0013770	10.9900	0.0013800	12.5800	0.0014960				
4	2.9900	0.0019390	6.1070	0.0015530	8.5820	0.0015500	10.6000	0.0016350				
5	3.6490	0.0017590	6.9910	0.0014620	9.7150	0.0014610	11.5600	0.0015620				
6	3.6490	0.0017590	6.9910	0.0014620	9.7150	0.0014610	11.5600	0.0015620				
7	7.3220	0.0005610	12.4100	0.0004980	17.1700	0.0004970	21.3000	0.0004752				
8	3.6490	0.0017590	6.9910	0.0014620	9.7150	0.0014610	11.5600	0.0015620				
9	6.1330	0.0006043	10.7800	0.0005248	15.0200	0.0005256	19.4100	0.0004970				
10	0.2072	0.0060240	1.9290	0.0036990	2.7760	0.0035360	3.3270	0.0035590				
11	0	0.0097710	0	0.0052580	0	0.0050270	0	0.0057860				
12	7.9090	0.0002725	13.4500	0.0002180	18.7600	0.0001981	23.4200	0.0001904				
13	3.6490	0.0017590	6.9910	0.0014620	9.7150	0.0014610	11.5600	0.0015620				

**Table 6**Optimization constraints of the SIGT–METVC system.

Subsystem	Parameter	Constraints	Reason
SIGT	HRSG outlet temperature	≥140 °C	To avoid formation of sulfuric acid in exhaust gases
	Turbine inlet temperature	≤1300	Material temperature limit
	SR	≥0.07	
	Net power generation	≥530 kW	Demand
METVC	$\Delta T_{METVC(3~effects)}$	2≤ΔT≤13	Temperature difference between First and last effect
	$\Delta T_{METVC~(4~effects)}$	$2 \le \Delta T \le 9$	Temperature difference between First and last effect
	$\Delta T_{METVC~(5~effects)}$	$2 \le \Delta T \le 6$	Temperature difference between First and last effect
	$\Delta T_{METVC~(6~effects)}$	$2 \le \Delta T \le 4$	Temperature difference between First and last effect
	Fresh water production	$\geq$ 10 m <sup>3</sup> /d	Demand

system. The central values chosen for the experimental design for  $\Delta T_{\rm METVC}$  were defined as 8 °C, 6 °C, 5 °C, and 4 °C and for SR as 0.077 kg/s, 0.0785 kg/s, 0.08 kg/s, and 0.0815 kg/s, in uncoded form for SIGT–METVC systems with 3, 4, 5, and 6 effects, respectively. By applying a multiple regression analysis on the design matrix (Table 5), the RSM models I, II, III, and IV were developed for SIGT–METVC systems with 3, 4, 5, and 6 effects (Table 7). These RSM models can be used to simulate SIGT–METVC systems in order to obtain  $Q_{\rm freshwater}$ 

The analysis of variance (ANOVA) is essential to test the significance of the developed models. Therefore, ANOVA was conducted to test the significance of the fit of the second-order polynomial equation for the RSM models on the coded equations (Table 8). The ANOVA of the regression models in Table 8 showed that the quadratic model was highly significant, as was evident from the Fisher's *F*-test with a very low probability value p-value. As presented in Table 8, for RSM model I, *F* value for Q<sub>freshwater</sub> and STECFW were 2,483,809.34 and 3458789.12, and the

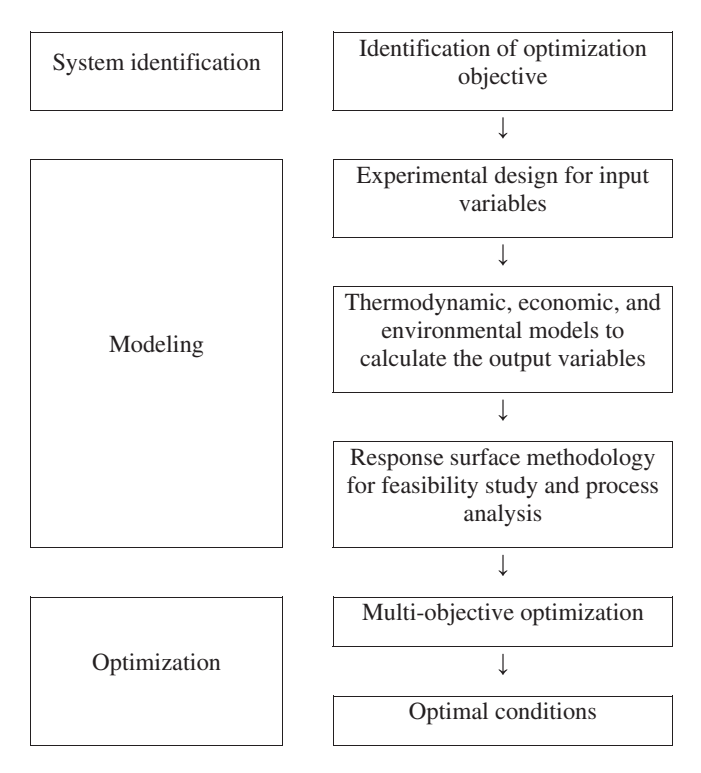


Fig. 5. Frame work of the SIGT-METVC system integration.

p-values were 0.000. On the other hand, Fisher's F-test was 2.915 and 3.011 which were calculated using MATLAB software. The calculated F values were found to be greater than the Fisher's F-test at the 5% level. As shown in Table 8, for RSM models II, III, and V, all of the F values were greater than Fisher's F-test at the 5% level and the P-values were 0.000. Since, in all of the RSM models, the calculated F values were greater than Fisher's F-test, the Fisher's F-test concluded with 95% certainly that the regression model explained a significant amount of the variation in the responses. The goodness of fit of the model was checked by the multiple correlation coefficients (R<sup>2</sup>). The values of R<sup>2</sup> for RSM models I, II, III and V are presented in Table 8. For RSM model I, the values of R<sup>2</sup> indicates that the regression model of Q<sub>freshwater</sub> explains most of the total variations. In addition, the values of the adjusted multiple correlation coefficient (adj. R2) (Table 8) were also very high, showing a high significant for the model. Similarly, for RSM models II, III and V, the R<sup>2</sup> and adj. R<sup>2</sup> were also very high, which indicate the goodness of fit of these models. As presented in Table 8 for RSM models I, II, III and V, for Q<sub>freshwater</sub> and STECFW the interaction effects occur between  $\Delta T_{METVC}$  and SR and also the main effect of SR is higher than main effect of  $\Delta T_{METVC}$ . It can be seen in Table 8 that  $\Delta T_{METVC}$  has quadratic effect on Qfreshwater while SR has quadratic effect on STECFW.

The response contour plots of  $Q_{freshwater}$  and STECFW as a function of two factors ( $\Delta T_{METVC}$  and SR) were plotted using the RSM models presented in Table 8. These plots are shown in Figs. 6a to d and 7a to d. In addition, since the net power generation is a function of the SR, the variations of  $W_{net}$  with respect to the SR are plotted in Fig. 6a to d for SIGT–METVC systems with 3, 4, 5, and 6 effects, respectively.

# 3.1.1. Sensitivity analysis and feasibility study for retrofitting the SIGT plant with METVC system

Fig. 6a to d shows the effect of the  $\Delta T_{METVC}$  and SR on the fresh water production and net power generation of the SIGT-METVC systems with 3, 4, 5, and 6 effects, respectively. As shown in Fig. 6, the effect of the SR on the fresh water production is higher than that of the  $\Delta T_{METVC}$ . This is because the variations of the fresh water production resulting from variations in the  $\Delta T_{\text{METVC}}$  at a fixed value of the SR were less than the variations of the fresh water production due to variations of the SR at a fixed value of SR  $\Delta T_{METVC}$ . The fresh water production increased as the SR decreased, because the required steam for injection into the combustion chamber decreased, resulting in a decrease in the fresh water consumption by the SIGT system. This then causes an increase in the fresh water production of the SIGT-METVC system. As seen in Fig. 6, the fresh water production increases with increases in  $\Delta T_{MFTVC}$ . This is due to the fact that the temperature of the first effect is fixed at 65 °C (presented in Table 2), and the last effect temperature of the METVC system decreases with increases in  $\Delta T_{METVC}$ . Therefore, more heat can be released in the METVC effects, which results in more fresh water

**Table 7**RSM models based on uncoded factors for SIGT–METVC system with 3, 4, 5, and 6 effects.

Model number	RSM model
I(n=3)	$\begin{aligned} &Q_{freshwater} = 46.577 + 0.478 \ \Delta T - 570.408 \ SR + 0.003 \ \Delta T^2 - 4.845 \ SR \\ &\Delta T \\ &STECFW = 0.0784 + 0.0009 \ \Delta T - 2.2919 \ SR + 16.7202 \ SR^2 - 0.0107 \\ &SR \ \Delta T \end{aligned}$
II (n=4)	$\begin{aligned} &Q_{freshwater} = 59.774 + 1.11 \; \Delta T - 693.095 \; SR + 0.008 \; \Delta T^2 - 11.281 \; SR \\ &\Delta T \\ &STECFW = 0.0784 + 0.0009 \; \Delta T - 2.2919 \; SR + 16.7202 \; SR^2 - 0.0107 \\ &SR \; \Delta T \end{aligned}$
III $(n=5)$	$Q_{freshwater} = 70.579 + 2.229 \Delta T - 792.786 SR + 0.018 \Delta T^2 - 22.579 SR \Delta T$ $STECFW = 0.0489 + 0.001 \Delta T 1.465 SR + 10.8989 SR^2 - 0.0116 SR \Delta T$
V (n = 6)	$\begin{aligned} &Q_{freshwater} = 79.370 + 3.959 \ \Delta T - 874.309 \ SR + 0.033 \ \Delta T^2 - 39.629 \ SR \\ &\Delta T \\ &STECFW = 0.0588 + 0.001 \ \Delta T - 1.7371 \ SR + 12.6445 \ SR^2 - 0.0085 \ SR \\ &\Delta T \end{aligned}$

**Table 8**Results of ANOVA for RSM models.

	71 IOI KSIVI IIIOUC	.13.			
RSM model I (	(n = 3)				
$Q_{\text{fresh water}}$ $R^2 = 1$ , adj. $R^2$	? = 1				
Source	Degree of	Sum of	Mean	F-value	P-
	freedom	squares	square		value
Regression	4	75.6021	18.9005	2483809.34	0.000
Residual Total	8 12	0.0001 75.6022	0.0000		
Term	ect and coefficier Effect	its Coef	SE coef	T	P
Constant	Lifect	46.577	0.050639	919.788	0.000
ΔΤ	0.956	0.478	0.006160	77.581	0.000
SR	-1140.816	-570.408	0.654148	-871.987	0.000
$\Delta T^2$ $\Delta T \cdot SR$	0.006 9.69	0.003 4.845	0.000083 0.078035	30.144 62.204	0.000
	- 3.03	-4,043	0.078033	-02,204	0.000
STECFW $R^2 = 99.6$ , adj	$P^2 - 99.1$				
Source	Degree of	Sum of	Mean	F-value	P-
	freedom	squares	square		value
Regression	5	81.235	15.568	3458789.12	0.000
Residual	7	0.0002 81.234	0.000		
Total	12				
Estimated effe Term	ect and coefficier Effect	nts Coef	SE coef	T	P
Constant	LIICU	0.3043	0.0629	4.8379	0.002
ΔΤ	0.0038	0.0019	0.0015	1.2667	0.001
SR	-17.228	-8.6141	1.6112	-5.3464	0.000
SR <sup>2</sup> ΔT · SR	121.687 0.047	60.8408 0.0235	10.4102 0.0191	5.8443 1.23	0.003
Δ1 SK	0,047	0.0233	0.0151	1.23	0.000
RSM model II	(n=4)				
$Q_{\text{fresh water}}$ $R^2 = 1$ , adj. $R^2$	2 — 1				
Source	Degree of	Sum of	Mean	F-value	P-
	freedom	squares	square		value
Regression	4	170.691	42.6727	2151261.91	0.000
Residual Total	8 12	0.000 170.691	0.0000		
Estimated effe Term	ect and coefficier Effect	its Coef	SE coef	T	P
Constant	Effect	59.774	0.08601	694.98	0.000
ΔΤ	2.22	1.11	0.014447	76.726	0.000
SR	-1386.19	-693.095	1.08265	-640.183	0.000
$\Delta T^2$ $\Delta T \cdot SR$	0.016 22.562	0.008 11.281	0.00037 0.17507	20.721 64.440	0.000
	22,002	111201	0,17507	0 11 110	0.000
STECFW R <sup>2</sup> = 99.9, adj	$R^2 = 99.8$				
Source	Degree of	Sum of	Mean	F-value	P-
	freedom	squares	square		value
Regression Residual	5 7	183.2548 0.000	52.3654 0.0002	2458987.25	0.000
Total	12	183.255	0.0002		
	ect and coefficier				
Estimated effe Term	Effect	Coef	SE coef	T	P
Constant	•	0.0784	0.01322	5.93	0.001
ΔΤ	0.0018	0.0009	0.00063	1.376	0.000
SR SR <sup>2</sup>	-4.5838 33.4404	-2.2919 16.7202	0.32553 2.0513	7.040 8.151	0.001 0.000
ΔT · SR	-0.0214	-0.0107	0.00768	-1.388	0.000
RSM model III	(n=5)				
$Q_{\text{fresh water}}$ $R^2 = 1$ , adj. $R^2$	$^{2} = 1$				
Source	Degree of	Sum of	Mean	F-value	P-
ъ .	freedom	squares	square	0.4.46800000	value
Regression Residual	4 8	330.892 0.000	82.7229 0.0003	2446700.33	0.000
Total	12	330.892	0.0003		
	ect and coefficier				
Term	Effect	Coef	SE coef	T	P
Constant		70.579	0.12276	574.949	0.000
ΔΤ	4.458	2.229	0.02595	85.849	0.000

Table 8 (continued)

able 8 (continu					
RSM model I (	(n=3)				
SR	-1585.572	-792.786	1.49684	-529.639	0.000
$\Delta T^2$	0.036	0.018	0.00109	16.557	0.000
$\Delta T \cdot SR$	-45.158	-22.579	0.29362	-76.960	0.000
STECFW					
$R^2 = 0.99$ , adj	$R^2 = 0.985$				
Source	Degree of	Sum of	Mean	F-value	P-
	freedom	squares	square		value
Regression	5	425.254	93.587	29874587.25	0.000
Residual	7	0.000	0.000		
Total	12	425.255			
	ect and coefficier				
Term	Effect	Coef	SE coef	T	P
Constant		0.0489	0.00955	5.124	0.001
ΔΤ	0.002	0.001	0.0008	1.263	0.000
SR	-2.93	-1.465	0.22242	-6.589	0.001
SR <sup>2</sup>	21.7978	10.8989	1.3603	8.013	0.002
$\Delta T \cdot SR$	-0.0232	-0.0116	0.00901	-1.286	0.000
RSM model V	(n = 6)				
Q <sub>fresh water</sub>	,				
$R^2 = 1$ , adj. $R^2$	$^{2} = 1$ , Fisher's <i>F</i> -1	test = 2.915			
Source	Degree of	Sum of	Mean	F-value	P-
	freedom	squares	square		value
Regression	4	560.236	140.05895	3190068.52	0.000
Residual	8	0.000	0.00004		
Total	12	560.236			
Estimated effe	ect and coefficier	ıts			
Term	Effect	Coef	SE coef	T	P
Constant		79.370	0.2065	384.360	0.000
ΔΤ	7.918	3.959	0.06193	63.924	0.000
SR	-1748.618	-874.309	2.34886	-372,227	0.000
$\Delta T^2$	0.066				
		0.033	0.00497	6.614	0.000
$\Delta T \cdot SR$	-79.258	-39.629	0.00497 0.58271	6.614 68.008	0.000
STECFW	-79.258				
STECFW $R^2 = 0.98$ , adj	$-79.258$ $R^2 = 0.97$	-39.629	0.58271	-68.008	0.000
STECFW	$-79.258$ $R^2 = 0.97$ Degree of	-39.629 Sum of	0.58271 Mean		0.000 P-
STECFW R <sup>2</sup> = 0.98, adj Source	$-79.258$ $R^2 = 0.97$ Degree of freedom	-39.629 Sum of squares	0.58271 Mean square	-68.008 F-value	0.000 P- value
STECFW $R^2 = 0.98$ , adj Source Regression	$-79.258$ $R^{2} = 0.97$ Degree of freedom 5	-39.629 Sum of squares 570.365	0.58271 Mean square 142.2548	-68.008	0.000 P-
STECFW R <sup>2</sup> = 0.98, adj Source Regression Residual	$-79.258$ $R^2 = 0.97$ Degree of freedom $5$ $7$	-39.629 Sum of squares 570.365 0.000	0.58271 Mean square	-68.008 F-value	0.000 P- value
STECFW $R^2 = 0.98$ , adj Source Regression	$-79.258$ $R^{2} = 0.97$ Degree of freedom 5	-39.629 Sum of squares 570.365	0.58271 Mean square 142.2548	-68.008 F-value	0.000 P- value
STECFW $R^2 = 0.98$ , adj Source Regression Residual Total Estimated effects	$-79.258$ $R^2 = 0.97$ Degree of freedom $5$ $7$ $12$ ect and coefficier	-39.629  Sum of squares 570.365 0.000 570.365	0.58271 Mean square 142.2548 0.000	68.008 F-value 3250054.25	0.000 P- value 0.000
STECFW $R^2 = 0.98$ , adj Source Regression Residual Total Estimated effecterm	$-79.258$ $R^2 = 0.97$ Degree of freedom $5$ $7$ $12$	-39.629  Sum of squares 570.365 0.000 570.365 ats Coef	0.58271 Mean square 142.2548 0.000	-68.008  F-value 3250054.25	0.000 P- value 0.000
STECFW  R <sup>2</sup> = 0.98, adj  Source  Regression  Residual  Total  Estimated effe  Term  Constant	-79.258  R <sup>2</sup> = 0.97 Degree of freedom 5 7 12 ect and coefficien	-39.629  Sum of squares 570.365 0.000 570.365 ats Coef 0.0588	0.58271 Mean square 142.2548 0.000 SE coef 0.01753	-68.008  F-value 3250054.25  T 3.356	P- value 0.000
STECFW $R^2 = 0.98$ , adj Source Regression Residual Total Estimated effe Term Constant $\Delta T$	-79.258  R <sup>2</sup> = 0.97 Degree of freedom 5 7 12 ect and coefficient Effect 0.002	-39.629  Sum of squares 570.365 0.000 570.365  its Coef 0.0588 0.001	0.58271  Mean square 142.2548 0.000  SE coef 0.01753 0.00147	-68.008  F-value 3250054.25  T 3.356 0.704	P-value 0.000 P 0.000 0.000
STECFW $R^2 = 0.98$ , adj Source Regression Residual Total Estimated effet Term Constant $\Delta T$ SR	-79.258  R <sup>2</sup> = 0.97 Degree of freedom 5 7 12 ect and coefficient Effect 0.002 $-3.4742$	- 39.629  Sum of squares 570.365 0.000 570.365 ats  Coef 0.0588 0.001 - 1.7371	0.58271  Mean square 142.2548 0.000  SE coef 0.01753 0.00147 0.40849	- 68.008  F-value 3250054.25  T 3.356 0.704 - 4.252	P-value 0.000 P 0.000 0.000 0.002 0.001
STECFW $R^2 = 0.98$ , adj Source Regression Residual Total Estimated effectors Constant $\Delta T$	-79.258  R <sup>2</sup> = 0.97 Degree of freedom 5 7 12 ect and coefficient Effect 0.002	-39.629  Sum of squares 570.365 0.000 570.365  its Coef 0.0588 0.001	0.58271  Mean square 142.2548 0.000  SE coef 0.01753 0.00147	-68.008  F-value 3250054.25  T 3.356 0.704	P-value 0.000 P 0.000

production. However the heat transfer area of the METVC effects increased, causing increases in the capital costs of the METVC systems.

Fig. 7a to d shows the effect of the  $\Delta T_{METVC}$  and SR on the STECFW of the SIGT–METVC systems with 3, 4, 5, and 6 effects, respectively. As shown in Fig. 7, the effect of the  $\Delta T_{METVC}$  on the STECFW at the fixed SR value is less than that of the SR on the STECFW at fixed value of the  $\Delta T_{METVC}$ . As the SR increases, the STECFW increases since the required fuel maintaining the turbine inlet temperature increases and then leads to the increase of the STECFW of the SIGT–METVC system. As seen in Fig. 7 the STECFW at the fixed value of the SR decreases with the increases in  $\Delta T_{METVC}$ . As explained in Fig. 6, the increase of  $\Delta T_{METVC}$  leads to the increase of the fresh water production, which results in the decrease of the fuel consumption of the SIGT–MEE system.

Fig. 6 demonstrates the possibility of the retrofitting the SIGT system (presented in Table 1) with the METVC system (presented in Table 2). According to Table 6, the SIGT–METVC systems are feasible, capable of producing fresh water and power exceeding  $10\,\mathrm{m}^3$ /day and  $530\,\mathrm{kW}$ , respectively, while satisfying the other constraints. Fig. 6a shows that the SIGT–METVC system with 3 effects was capable of producing fresh water up to approximately  $9\,\mathrm{m}^3$ /day and could generate power up to

around 539.7 kW. Since the SIGT-METVC system with 3 effects cannot produce fresh water exceeding 10 m<sup>3</sup>/d, which is the minimal desirable value for water production, retrofitting the SIGT system with a METVC system with 3 effects is not feasible, despite power generation being satisfied by this system. Fig. 6b to d shows that the SIGT-METVC system with 4, 5, and 6 effects can produce fresh water exceeding 10 m<sup>3</sup>/d and can generate power of more than 530 kW, which exceed the minimal desirable values of fresh water and power production. The highlighted areas in Fig. 6b to d represent feasible operation conditions for the integration of the SIGT and METVC systems. These feasible areas depicted are defined by four bounds, including a left bound which represents the operation conditions for power generation of 530kW, a right bound which represents the operation conditions for fresh water production of 10 m<sup>3</sup>/day, an upper bound which is defined based on the maximum possible value of the  $\Delta T_{METVC}$  (presented in Table 6), and a lower bound which represents the power generation values. An increase in the number of effects in the METVC system increases the area of the feasible region. Because fresh water production increases with increased numbers of effects, the fresh water production values corresponding to the left bound operation conditions also increase with increased numbers of effects. Increasing the total amount of fresh water produced by SIGT-METVC system causes increases in the injected steam flow rate, which leads to increased power generation. Therefore, the lower bound, which represents the net power generation of the SIGT-METVC system, increases with increased numbers of effects, which thereby increases the feasible area for the SIGT-METVC system. These results show that increasing the number of effects causes increases in the net fresh water production, and SR, which increases the net power generation and CO emissions, and decreases the NOx emissions. In addition, increasing the number of effects results in increases in the capital costs of the METVC system. Therefore, optimization should be performed in order to determine the optimal number of effects with the respective economic and environmental considerations.

# 3.2. Multi-objective optimization

Optimization was carried out to minimize the RUPC of the SIGT–METVC systems with 3, 4, 5, and 6 effects by minimizing the RTAC and maximizing the  $Q_{fresh\ water}$ . The Pareto optimal solution, obtained by using GA for the MOO so as to minimize the RTAC and to maximize the  $Q_{fresh\ water}$  for SIGT–METVC systems with 4, 5, and 6 effects are presented in Fig. 8a to c, respectively. The Pareto optimal solution for SIGT–METVC system with three effects was not achieved through GA because the feasibility study results showed that the retrofitting the SIGT with METVC system with three effects is impossible.

Each point of the Pareto set (comprising the RTAC and  $Q_{fresh\ water}$ ) is associated with a set of input decision variables (a set of  $\Delta T_{METVC}$  and SR). In order to select the best point among the Pareto solution points, the values of the RUPC corresponding to each Pareto front were calculated using Eq. (15). The RUPC that corresponds to each Pareto point is shown in Fig. 8a to c for SIGT–METVC systems with 4, 5, and 6 effects in the METVC system. Since the purpose of the optimization was to minimize the RUPC, the Pareto front that corresponded to the minimum

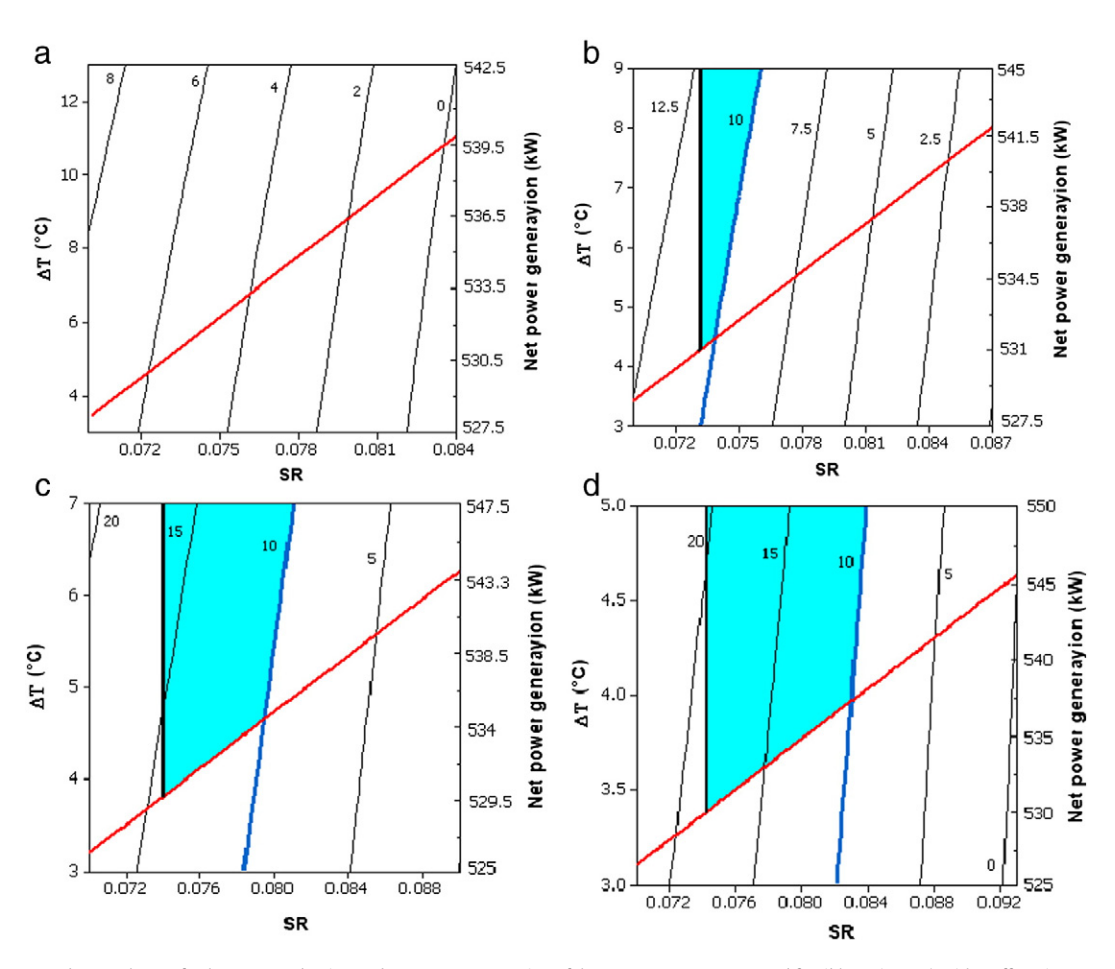


Fig. 6. Effect of  $\Delta T_{METVC}$  and SR on the net fresh water production and net power generation of the SIGT–METVC system and feasible regions: a) with 3 effects in METVC system b) with 4 effects in METVC system c) with 5 effects in METVC system d) with 6 effects in METVC system.

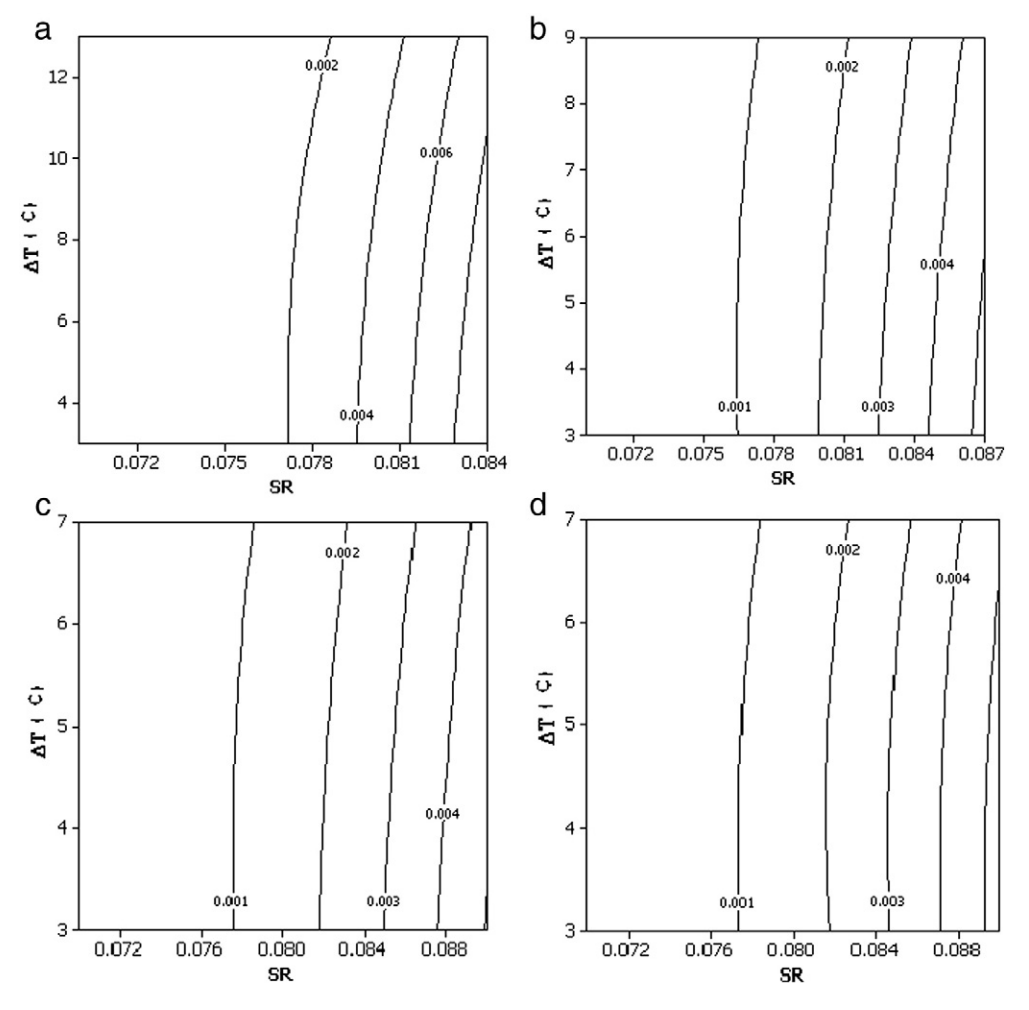


Fig. 7. Effect of ΔT<sub>METVC</sub> and SR on the specific thermal energy cost of fresh water (STECFW) of the SIGT–METVC system a) with 3 effects in METVC system b) with 4 effects in METVC system b) with 6 effects in METVC system d) with 6 effects in METVC system.

RUPC was selected as the best operation point. However, all of the Pareto fronts represent operation conditions with a minimum RUPC, but with different net fresh water production. The selected points are shown with an arrow in Fig. 8. The optimization results for SIGT–METVC systems with 4, 5, and 6 effects, where the operation was based on the selected points, are presented in Table 9.

As seen in Table 9, increasing the number of effects in the METVC desalination system caused the values of Q<sub>fresh water</sub>, W<sub>net</sub> and SR to increase, while the SIGT-METVC system with 5 effects had the minimum RUPC value among the other systems. This can be explained by Eq. (15), which calculates the RUPC by dividing the RTAC by Q<sub>fresh</sub> water. As the number of effects increases from 4 to 5, the Qfresh water increases higher than RTAC, which decreases the value of RUPC. As the number of effects increases from 5 to 6, the Qfresh water does not increase as much as the RTAC. This can be explained by Eq (16), which calculates the RTAC based on four terms: the TAC<sub>METVC</sub>, LOCPG, LOCNO<sub>x</sub>, and FOCCO. Furthermore, the RTAC decreases with an increased number of effects, from 4 to 5. However, increasing the TAC<sub>METVC</sub> by increasing the number of effects is less than the effect from decreasing the LOCPG and LOCNO<sub>x</sub> and increasing the FOCCO, due to the increased SR. The RTAC increased with an increase in the number of effects, from 5 to 6. The effect of increasing the  $TAC_{METVC}$  due to an increase in the number of effects is higher than the effect from decreasing the LOCPG and LOCNO<sub>x</sub> and increasing the FOCCO. Therefore, the RTAC value of the SIGT-METVC system with 5 is less than that of the SIGT- METVC system with 4 and 6 effects. Based on the summarized results in Table 9, the SIGT–METVC system with 5 effects may reduce the RUPC by 21.07% and 9.54%, compared to systems with 4 and 6 effects, respectively. In addition, the system with 5 effects was capable of increasing the net fresh water production and net power generation by 15.1% and 0.2% compared to the system with 4 effects. The sets of input decision variables corresponding to the points selected as design parameters are tabulated in Table 9. As seen there, the values of the  $\Delta T_{\rm METVC}$  and SR corresponding to the best Pareto point for a system with 5 effects are 6.8 °C and 0.0776 kg/s, which we determined to be the optimal design parameters.

#### 4. Conclusions

In this study, we retrofitted a SIGT plant with a METVC desalination system to cogenerate fresh water and power, analyzing and optimizing the process. The primary conclusions drawn from the present study are listed as follows:

1—A new performance criterion for retrofitting a SIGT plant with METVC desalination was proposed by considering the thermodynamic, economic, and environmental aspects in the calculations of the unit product cost of the fresh water as the retrofitted unit product cost of the fresh water (RUPC).

2—The influences of the steam air ratio (SR) and temperature difference between the effects of the METVC system ( $\Delta T_{METVC}$ ) as the two key

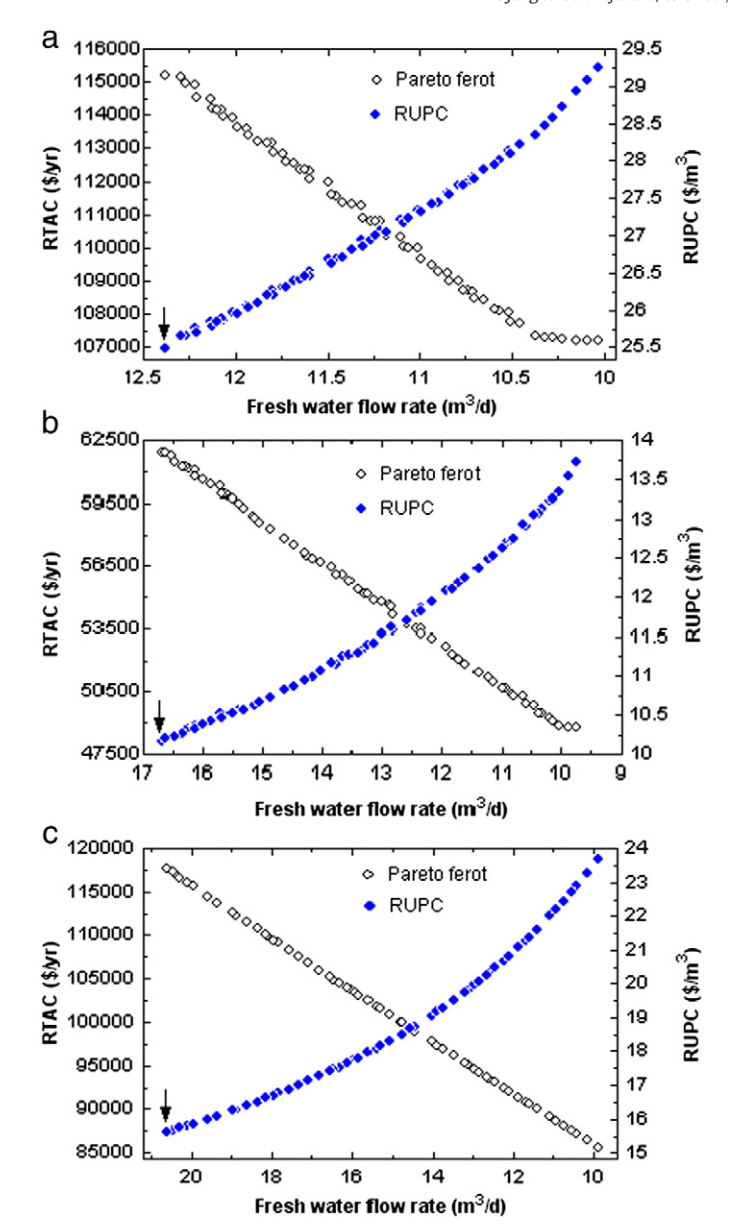


Fig. 8. Pareto optimal solutions for RTAC, and  $Q_{fresh\ water}$ , using multi-objective optimization, as well as MUPC, corresponding to each pareto point a: for SIGT-METVC system with 4 effects, b: for SIGT-METVC system with 5 effects, c: for SIGT-METVC system with 6 effects.

parameters on the net fresh water production Q<sub>freshwater</sub> and net power generation (W<sub>net</sub>) of the SIGT-METAC systems with 3, 4, 5, and 6 effects were analyzed and the feasibility of the SIGT-METVC system was studied using response surface methodology (RSM).

3-Multi-objective optimization was carried out to optimize the RUPC. Among the SIGT-METVC systems, the system with 5 effects was

Input decision variables corresponding to each of the preferred points, as depicted in Fig. 6.

Effects no.	RUPC (\$/m³)	Q <sub>freshwater</sub> (m <sup>3</sup> /day)	W <sub>net</sub> (kW)	RTAC (\$/yr)	ΔT <sub>METVC</sub> (°C)	SR
n = 4	21.02	11.24	531.8	86,236	8.87	0.0744
n = 5	16.59	13.24	534.6	80,173	6.8	0.0776
n = 6	18.34	15.1	537.2	101.081	5	0.0791

selected as the best system with the minimum value of the RUPC at  $16.59 (\$/m^3)$ .

Nomenclature

**Abbreviations** 

AC Air compressor ACC Annual capital cost, \$/yr AOC Annual operating cost, \$/yr

**APH** Air pre-heater

**BPE** Boiling point evaluation, °C CCCombustion chamber CCD Central composite design CHP Combined heat and power CO Carbone monoxide DOE Design of experiment **EvGT** Evaporative gas turbine **FOCCO** Found opportunity cost of CO

GA Genetic algorithm GT Gas turbine HAT Humid air turbine Humid gas turbine **HGT** 

Heat recovery steam generator HRSG LHV Lower heating value, kI/kg

**LMTD** Logarithmic mean temperature difference LOCPG Lost opportunity cost of power generation

LOCNO<sub>x</sub> Lost opportunity cost of NO<sub>x</sub>

**METVC** Multi effects distillation-thermal vapor compression

MOO Multi-objective optimization NEA Non-equilibrium allowance

 $NO_x$ Nitrogen oxide TAC Total annual cost, \$/yr

**RTAC** Retrofitted Total annual cost, \$/yr Response surface methodology **RSM RUPC** Retrofitted unit product cost, \$/m<sup>3</sup> **SIGT** Steam-injected gas turbine

SJE Steam jet ejector SP Sale price

Specific thermal energy cost of fresh water, \$/m<sup>3</sup> **STECFW** 

**UPC** Unit product cost, \$/m3

Symbols

r

Α Heat transfer area, m<sup>2</sup>

AF Air fuel ration

В Brine blow down mass flow rate, kg/s

C

 $C_{p}$ Specific heat capacity, kJ/kg°C

D Distillate, kg/s F Feed flow rate, kg/s f Plant load factor

Н Inferior caloric value of the fuel, kcal/kg

h Specific enthalpy, kJ/kg L Latent variable Mass flow rate, kg/s m

Number of effects in MED-TVC system n

P Pressure, kPa T Temperature, °C

T Temperature of brine in each effect

Compression ratio SR Steam air ratio

Ŧ Temperature of brine after cooling U Heat transfer coefficient, kW/m<sup>2</sup>k

W Power, MW Χ Salinity, ppm Flashing fraction у Y Response

Z Amortization factor, 1/yr

#### Subscripts

a	air
b	building
0	Reference point
CI	Capital investment
Con	Condenser

D Destructed effect e engineer en Electricity el Feed water f Flue gas g

Heater Index of component K

L labor

Н

Primary zone Pz returned r Reference ref steam S seawater SW

transportation tr

# Greek

В Regression coefficient Specific heat ratio  $\gamma$ 

Gradient Δ Efficiency η

Dimension less pressure θ

λ Air exec coefficient for a minimum air quantity

Saturated vapor

Heat emission coefficient ξ Dimension less pressure π

Residence time in the combustion zone

Mass or molar ratio φ

Atomic ratio

# Acknowledgments

This work was supported by the Korea Science and Engineering Foundation (KOSEF) grant funded by the Korean government (MEST) (KRF-2012-001400) and also by the National Research Foundation of Korea (NRF) grant funded by the Korea government (MSIP) (No. 2008-0061908).

# Appendix A. Thermodynamic models for GT power plant and METVC desalination system

Table 1A Governing equations for the thermodynamic modeling of the gas turbine power plant [15,16].

0 1	0 1 1	
Equations	Description	
$T_2 = T_1 \tilde{n} \left( 1 + \frac{1}{\eta_{AC}} \left( r_{AC} \frac{\gamma_0 - 1}{\gamma_0} - 1 \right) \right)$	Outlet temperature of an air compressor	(A1)
$W_{AC} = \dot{m}_a C_{pa} (T_2 - T_1)$	Power consumption of an	(A2)
$C_{pa}(T) = 1.04841 - \left(\frac{3.8371T}{10^4}\right) + \left(\frac{9.4537T^2}{10^7}\right) - \left(\frac{5.49031T^3}{10^{10}}\right)$	air compressor Heat capacity of air	(A3)
$+\left(\frac{7.92987^4}{10^{14}}\right)$	Energy balance	(A4)
$\dot{m}_a h_3 + \dot{m}_{fuel} LHV + \dot{m}_{water} h_{water} = \dot{m}_g h_4$	equation of a combustion	
$+(1-\eta_{cc})\dot{m}_{fuel}LHV+\dot{m}_{water}h_{steam}$	chamber	
$\dot{m}_g = \dot{m}_a + \dot{m}_{fuel}$	Mass balance equation of a combustion chamber	(A5)

Table 1A (continued)

Equations	Description	
$\frac{\frac{P_4}{4}}{\frac{1}{P_3}} = (1 - \Delta P_{cc})$	Pressure drop in the combustion chamber	(A6)
$T_5 = T_4 \left( 1 - \eta_{GT} \left( 1 - \left( \frac{P_4}{P_5} \right)^{\frac{1 - \gamma_g}{\gamma_g}} \right) \right)$	Outlet temperature of a gas turbine	(A7)
$C_{pg}(T) = 0.991615 + \left(\frac{6.99703T}{10^5}\right) + \left(\frac{2.7129T^2}{10^7}\right) - \left(\frac{1.22427T^3}{10^{10}}\right)$	Heat capacity of flue gas	(A8)
$\dot{m}_{\mathbf{d}}(h_3 - h_2) = \dot{m}_{\mathbf{g}}(h_5 - h_6) \cdot \eta_{APH}$	The energy balance equation of an air pre-heater	(A9)
$\frac{P_3^3}{P_2} = (1 - \Delta P_{APH})$	A pressure drop in the air pre-heater	(A10)
$\dot{m}_{g}(h_{9}-h_{8}) = \dot{m}_{g}C_{pg}(T_{6}-T_{7})$	The energy balance equation of the HRSG	(A11)
$\dot{m}_{water} = rac{\xi H_{fiel} + \lambda AF(h_3 - h_1) - (\lambda AF + 1)(h_4 - h_1)}{h_{steam} - h_{water}}  \dot{m}_{fiel}$	Mass flow rate of water injection	(A12)
$W_{GT} = (\dot{m}_{water} + \dot{m}_g)C_{pg}(T_4 - T_5)$	GT power generation	(A13)
$\dot{W}_{net} = \dot{W}_{GT} - \dot{W}_{AC}$	Net power generation	(A14)

Table 2A Mass, salinity, and energy balance equations for each of the effects in the METVC system [3].

Equations	Descriptions	
$B_1 = F_1 - D_1$	Mass balance of effect 1	(A15)
$B_{i} = F_{i} + B_{i-1} - D_{i} + \left[ y_{i-1} \tilde{n} \left( D_{r} + \sum_{j=1}^{i-2} D_{j} \right) \right] - \left[ (i-1)\tilde{n} F_{i-1} \tilde{n} y_{i-1} \right]$	Mass balances of effects 2 to n	(A16)
$D_{\text{con.}} = D_n - {}^n D_r + \left[ y_n \tilde{n} \left( D_r \tilde{n} \sum_{i=1}^{n-1} D_i \right) \right]$	Mass balance of end	(A17)
$D = \left[ (1 - y_n) \hat{n} \left( D_r + \sum_{i=1}^{n-1} D_i \right) \right] - \left[ y_{n-1} \left( D_r + \sum_{i=1}^{n-2} D_i \right) \right] - \left[ y_{n-3} \left( D_r + \sum_{i=1}^{n-4} D_i \right) \right]$	condenser	()
$-\left[y_{n-4}\left(D_r + \sum_{i=1}^{n-5} D_i\right)\right] - (y_{n-5}\tilde{n}D_r) + D_{con}.$	Mass balance of Distillate tank	(A18)
$X_{sw}\tilde{n}F_1=X_{B_1}\tilde{n}B_1$	Salinity	(A19)
v ar . (v an ) v an	balance of effect 1 Salinity	(A20)
$X_{sw} \hat{n} F_i + \left( X_{B_{i-1}} \hat{n} B_{i-1} \right) = X_{B_i} \hat{n} B_i$	balance of effects 2 to n	(A20)
$D_1 \tilde{n} L_1 + (F_1 \tilde{n} C_p (T_1 - T_{f_1})) = m_0 \tilde{n} L_0$	Energy balance	(A21)
$\begin{split} &D_{i} \tilde{n} L_{i} + \left[ F_{i} \tilde{n} C_{p} (T_{i} - T_{f_{i}}) \right] = (D_{i-1} \tilde{n} L_{i-1}) + \left[ y_{i-1} \tilde{n} \left( D_{r} + \sum_{j=1}^{i-2} D_{j} \right) \tilde{n} L_{i-1} \right] \\ &- \left[ (i-1) \tilde{n} F_{i-1} \tilde{n} y_{i-1} \tilde{n} L_{i-1} \right] + \left[ B_{i-1} \tilde{n} C_{p} \tilde{n} \left( T_{i-1} - \overline{T}_{i} \right) \right] \end{split}$	of effect 1 Energy balance of effects 2 to n	(A22)

Heat transfer area, heat transfer coefficient, and logarithmic mean temperature difference equations [3].

Equations	Description	
$A_{e1} = \frac{m_0 \bar{n}^0 L_0}{U_{e1} \bar{n} (T_{oc} - T_1)}$	Heat transfer area of effect 1	(A23)
$A_{ei} = \frac{\left[D_{i-1} + \left(\left(D_{r} + \sum_{j=1}^{i-2} D_{j}\right) y_{i-1}\right) - ((i-1)\bar{n}y_{i-1}\bar{n}F_{i})\right]\bar{n}L_{i-1}}{U_{d}(T_{i_{i-1}} - T_{i})}\right]\bar{n}L_{i-1}}{U_{d}(T_{i_{i-1}} - T_{i})}$	Heat transfer area of effects 2 to n	(A24)
$A_{total} = \sum_{i=1}^{n} A_i$	Total heat transfer area of effects	(A25)
$A_{H_i} = \frac{\left(i\bar{n}F_i\bar{n}c\bar{n}\left(T_{f_i} - T_{f_{i+1}}\right)\right)}{U_{H_i}\bar{n}LMD_{H_i}}$	Heat transfer area of pre-heaters 1 to $n-1$	(A26)
$A_{H_n} = \frac{\left(\frac{n\tilde{n}F_n\tilde{n}C\tilde{n}(T_{f_n} - T_f)}{U_{H_n}\tilde{n}LMTD_{H_n}}\right)}{\left(\frac{n-1}{n-1}\right)}$	Heat transfer area of pre-heater n	(A27)
$A_{con.} = \frac{\left[D_{con.} + \left(\left(D_{r} + \sum_{j=1}^{n-1} Dj\right) \bar{\eta} y_n\right)\right] \bar{n} L_n}{U_{con.} \bar{n} L M D_{con.}}$	Heat transfer area of end condenser	(A28)

Table 3A (continued)

Equations	Description	
$U_{e1} = 1.9394 + \left(1.40562\tilde{n}10^{-3}\right)\tilde{n}T_{0c} - \left(2.07525\tilde{n}10^{-5}\right)\tilde{n}T_{0c} + \left(2.3186\tilde{n}10^{-6}\right)\tilde{n}T_{0c}^{3}$	Heat transfer coefficient of effect 1	(A29)
$U_{ei} = 1.9394 + \left(1.40562\tilde{n}10^{-3}\right)\tilde{n}T_{v_{i-1}} - \left(2.07525\tilde{n}10^{-5}\right)\tilde{n}T_{v_{i-1}} + \left(2.3186\tilde{n}10^{-6}\right)\tilde{n}T_{v_{i-1}}^{-3}$	Heat transfer coefficient of effects 2 to n	(A30)
$\begin{array}{l} U_{H_i} = 14.18251642 + 0.011383865 T_{v_i} \\ + 0.013381501 T_{f_{i-1}} \end{array}$	Heat transfer coefficient of pre- heaters 1 to n — 2	(A31)
$U_{H_{n-1}} = 14.18251642 + 0.011383865T_{v_{n-1}} + 0.013381501T_f$	Heat transfer coefficient of pre-	(A32)
$\begin{split} &U_{\text{cont.}} = 1.6175 + \left(1.537\bar{n}10^{-4}\right)T_{\nu_n} - \left(1.825\bar{n}10^{-4}\right)T_{\nu_n} \\ &+ \left(8.026\bar{n}10^{-8}\right)T_{\nu_n}{}^3 \end{split}$	heaters n — 1 Heat transfer coefficient of end	(A33)
$LMTD_{H_i} = \frac{\left(T_{I_i} - T_{I_{i+1}}\right)}{\ln\left(\frac{T_{i_0} - T_{I_{i+1}}}{T_{i_0} - T_{I_{i+1}}}\right)}$	condenser Logarithmic mean temperature difference of effects 1	(A34)
$LMTD_{H_{n-1}} = \frac{(r_{f_{n-1}} - r_f)}{\ln\left(\frac{r_{g_{n-1}} - r_f}{r_{g_{n-1}} - r_f}\right)}$	to n – 2 Logarithmic mean temperature difference of effect	(A35)
$LMTD_{con.} = \frac{(T_f - T_{so})}{\ln\left(\frac{T_{fin} - T_{fin}}{T_{fin} - T_f}\right)}$	n – 1 Logarithmic mean temperature difference of end condenser	(A36)

**Table 4A**Temperature profile equations of METVC desalination system [13].

Equations	Descriptions	
$T_i = T_{\nu_i} + (BPE)_i + \Delta T_{y_i}$	Saturated vapor temperature of effects	(A37)
$T_{ci} = T_{v_i} + \Delta T_{p_i}$	Vapor condensation temperature of effects	(A38)
$\overline{T}_1 = T_{0c} + NEA_1$	Flashing vapor condensation temperature of effect 1	(A39)
$\overline{T}_i = T_{v_i} + NEA_i$	Flashing vapor condensation temperature of effects	(A40)
	2 to n	
$T_{i}^{'} = T_{i} + NEA_{i}$	Flashing brines temperature of effects 2 to n	(A41)
$NEA_i = \frac{\left(0.33\tilde{n}(T_{i-1} - T_i)^{0.55}\right)}{T_{\nu_i}}$	Non-equilibrium allowance	(A42)

# Appendix B. Economic models for HRSG and METVC desalination system

**Table 1B**Economic model equations for METVC system for the calculations of the capital and operating costs [13].

Equations	Descriptions	
Capital costs		
$C_A = 140 \cdot A_E$	Area cost (\$)	(B1)
$C_{equipment} = 4 \cdot C_A$	Instrument cost	(B2)
	(evaporator, condenser) (\$)	
$C_{site} = 0.2 \cdot C_{eq}$	Site cost (\$)	(B3)
$C_{tr} = 0.05 \cdot (C_A + C_{eq} + C_s)$	Transportation costs (\$)	(B4)
$C_b = 0.15 \cdot C_{eq}$	Building costs (\$)	(B5)
$C_{en} = 0.1 \cdot C_{eq}$	Engineers and salary costs (\$)	(B6)
$C_c = 0.1 \cdot (C_A + C_{eq} + C_s)$	Contingency costs (\$)	(B7)
CC =	Capital costs (\$)	(B8)
$C_A + C_{equipment} + C_{site} + C_{tr} + C_b + C_{en} + C_{-}$		
$Z = \frac{(i(i+1)^n}{(i+1)^n}$ $ACC = CC \cdot Z$	Amortization factor Capital annual costs (\$/yr)	(B9) (B10)

Table 1B (continued)

Equations	Descriptions	
Operating Cost		
$C_{el} = c_{el} \cdot P \cdot f \cdot Q \cdot 365$	Electricity (\$/yr)	(B11)
$C_l = 0.1 \cdot f \cdot Q \cdot 365$	Labor cost (\$/yr)	(B12)
$C_{ch} = 0.04 \cdot f \cdot Q \cdot 365$	Chemical material costs (\$/yr)	(B13)
$C_{in} = 0.005 \cdot C_A$	Insurance costs (\$/yr)	(B14)
$AOC = C_{th} + C_{el} + C_l + C_{ch} + C_{in}$	Annual operating costs	(B15)

The capital cost of HRSG can be calculated by Eq. (B18). [18].

$$\textit{C}_{\textit{HRSG}} = \textit{c}_{41} \cdot \sum_{\textit{i}} \left( f_{\textit{p,i}} \cdot f_{\textit{T.Steam,i}} \cdot f_{\textit{T.gas,i}} \cdot \left( \frac{\textit{Q}}{\Delta T_{\textit{ln,i}}} \right)^{0.8} \right) + \textit{c}_{42} \cdot \sum_{\textit{j}} f_{\textit{p,j}} \cdot \dot{\textit{m}}_{\textit{team,j}} + \textit{c}_{43} \cdot \textit{m}_{\textit{gas}}^{1.2} \right)$$

where,  $f_{p,i}$ ,  $f_{T,steam,i}$ ,  $f_{T,gas,i}$ ,  $C_{41}$ ,  $C_{42}$ , and  $C_{43}$  are given by Eqs. (B19)–(B24). [18]

$$f_{p,i} = 0.0971 \cdot \frac{p_i}{30bar} + 0.9029$$

$$f_{T,steam,i} = 1 + \exp\left(\frac{T_{out,steam,i} - 830K}{500K}\right)$$

$$f_{T,gas,i} = 1 + \exp\left(\frac{T_{out,gas,i} - 990K}{500K}\right)$$

$$c_{41} = 413.8 \cdot (kW \cdot K)^{0.8}$$

$$c_{42} = 13380 \cdot (kg \cdot s)^{-1}$$

$$c_{43} = 1489.7 \cdot (kg \cdot s)^{-1.2}$$

#### References

- [1] G.M. Zak, A. Ghobeity, M.H. Sharqawy, A. Mitsos, A review of hybrid desalination systems for co-production of power and water: analysis, methods, and considerations, Desalin. Water Treat. (2013) 1–21.
- [2] Y. Wang, N. Lior, Fuel allocation in combined steam-injected gas turbine and thermal seawater desalination system, Desalination 214 (2007) 306–326.
- [3] Y. Wang, N. Lior, Performance analysis of combined humidified gas turbine power generation and multi-effect thermal vapor compression desalination systems— Part 1: the desalination unit and its combination with a steam-injected gs power system, Desalination 196 (2006) 84–104.
- [4] K. Nishida, T. Takagi, S. Kinoshita, Regenerative steam-injection gas-turbine systems, App. Energy. 81 (2005) 231–246.
- [5] S. Goke, M. Furi, G. Bourque, B. Bobusch, K. Gockeler, O. Kruger, S. Schimek, S. Terhaar, C.O. Paschereit, Fuel Process. Technol. 107 (2013) 14–22.
- [6] M.D. Paepe, E. Dick, Technological and economical analysis of water recovery in steam injected gas turbines, App. Therm. Eng. 21 (2001) 135–156.
- [7] Sh. Agarwal, S.S. Kachhwaha, R.S. Mishra, Performance improvement of a simple gas turbine cycle through integration of inlet air evaporative cooling and steam injection, J. Sci. Ind. Res. 70 (2011) 544–553.
- [8] J.J. Lee, M.S. Jeon, T.S. Kim, The influence of water and steam injection on the performance of a recuperated cycle microturbine for combined heat and power application, App. Energy 87 (2010) 1307–1316.
- [9] M. Cardu, M. Baica, Gas turbine installation with total water injection in the combustion chamber, Energy Conv. Manag. 43 (2002) 2395–2404.
- 10] H. Haselbacher, Performance of water/steam injected gas turbine power plants considering of standard gas turbines and turbo expanders, Int. J. Energy Technol. Policy 3 (2005) 12–23.
- [11] W.D. Paepe, F. Delattin, S. Bram, J.D. Ruyck, Steam injection experiments in a microturbine—a thermodynamic performance analysis, App. Energy 97 (2012) 569–576.
- [12] M. Salem Ahmed, H. Ahmed Mohamed, Performance characteristics of modified gas turbine cycles with steam injection after combustion exit, Int. J. Energy Res. 36 (2012) 1346–1357.
- [13] I. Janghorban Esfahani, A. Ataei, K.V. Shetty, T.S. Oh, J.H. Park, C.K. Yoo, Modeling and genetic algorithm-based multi-objective optimization of the METVC desalination system, Desalination 292 (2012) 87–104.
- [14] M. Shakouri, H. Ghadamian, R. Sheikholeslami, Optimal model for multi effect desalination system integrated with gas turbine, Desalination 260 (2010) 254–263.
- [15] I. Janghorban Esfahani, A. Ataei, M.J. Kim, O.Y. Kang, C.K. Yoo, Parametric analysis and optimization of combined gas turbine and reverse osmosis system using refrigeration cycle, Desalin. Water Treat. 43 (2012) 149–158.
- [16] Y. Wang, N. Lior, thermoeconomic analysis of a low-temperature multi-effect thermal desalination system coupled with an absorption pump, Energy 36 (2011) 3878–3887.
- [17] A. Lazzaretto, A. Toffolo, Energy, economy and environment as objectives in multi-criterion optimization of thermal systems design, Energy 29 (2004) 1139–1157.
- [18] P. Roosen, S. Uhlenbruck, K. Lucas, Pareto optimization of a combined cycle power system as a decision support tool for trading off investment vs. operating costs, Int. J. Therm. Sci. 42 (2003) 553–560.

- [19] I. Janghorban Esfahani, J.T. Kim, C.K. Yoo, A cost approach for optimization of a combined power and thermal desalination system through exergy and environmental analysis, Ind. Eng. Chem. Res. 52 (2013) 11099–11110.
- [20] K. Yetilmezsoy, S. Demirel, R.J. Vanderbei, Response surface modeling of pb(II) removal from aqueous by pistaciavera L.: Box-Behnken experimental design, J. Hazard. Mater. 171 (2009) 551–562.
- [21] P. Ahmadi, I. Dincer, M.A. Rosen, Exergy, exergoeconomic and environmental analyses and evolutionary algorithm based multi-objective optimization of combined cycle power plants, Energy 36 (2011) 5886–5898.
- [22] M.A. Bezerra, R.E. Santelli, E.P. Oliveria, L.S. Villar, L.A. Escaleria, Response surface methodology (RSM) as a tool for optimization in analytical chemistry, Talanta 76 (2008)
- [23] B. Sankararao, S.K. Gupta, Multi-objective optimization of an industrial fluidized-bed catalytic cracking unit (FCCU) using two jumping gene adaptations of simulated annealing, Comput. Chem. Eng. 31 (2007) 1496–1515.
- nealing, Comput. Chem. Eng. 31 (2007) 1496–1515.

  [24] M.J. Lee, Y.S. Kim, C.K. Yoo, J.H. Song, S.J. Hwang, Sewage sludge reduction and system optimization in a catalytic ozonation process, Environ. Technol. 31 (2010) 7–14.
- [25] D.C. Montgomery, G.C. Runger, N.F. Hubele, Engineering Statistics, forth ed. John Wiley & Sons, New Jersey, 2007.

- [26] I. Mohanty, D. Bhattacharjee, S. Datta, Desgning cold rolled IF steel with optimized tensile properties, Comput. Mater. Sci. 50 (2011) 2331–2337.
- [27] A. Konak, D.W. Coit, A.E. Smith, Multi-objective optimization using genetic algorithm: a tutorial, Reliab. Eng. Syst. Saf. 91 (2006) 992–1007.
- [28] N.K. Saxena, A. Khan, P.K.S. Pourush, N. Kumar, GA optimization of cutoff frequency of magnetically biased microstrip circular patch antenna, Int. J. Electron. (AEU) 65 (2011) 476–479
- [29] H.C. Liao, Using GA to dispatch the obtaining quantity for minimizing the total cost based on consideration of patient safety in HSCM, Expert Syst. Appl. 36 (2009) 11358–11362.
- [30] E.S. Elmolla, M. Chaudhuri, M.M. Hltoukhy, The use of artificial neural network (ANN) for modeling of COD removal from antibiotic aqueous solution by the Fenton process, J. Hazard. Mater. 179 (2010) 127–134.
- [31] M. Rajendra, P. Chandra Jena, H. Raheman, Prediction of optimization pretreatment process parameters for biodiesel production using ANN and GA, Fuel 88 (2009) 868–875.
- [32] M. Rayendra, J.P. Chandra, H. Raheman, Prediction of optimization pretreatment process parameters for biodiesel production using ANN and GA, Fuel 88 (2009) 868–875.
- [33] A. Konak, D.W. Coit, A.E. Smith, Multi-objective optimization using genetic algorithms: a tutorial, Reliab. Eng. Syst. Saf. 91 (2006) 992–1007.